Title
Early perturbation of Wnt signaling reveals patterning and invagination-evagination control points in molar tooth development

Author
Kim, Rebecca Yewon

Publication Date
2021

Peer reviewed|Thesis/dissertation

Early perturbation of Wnt signaling reveals patterning and invagination-evagination control points in molar tooth development

by
Rebecca Yewon Kim

DISSERTATION
Submitted in partial satisfaction of the requirements for degree of
DOCTOR OF PHILOSOPHY

in

Oral and Craniofacial Sciences

in the

GRADUATE DIVISION
of the
UNIVERSITY OF CALIFORNIA, SAN FRANCISCO

Approved:

DocuSigned by:
Bush, Jeffrey
367536768C42487...

Bush, Jeffrey
Chair

DocuSigned by:
Ophir Klein
DocuSigned by:
Torsten Wittmann
DocuSigned by:
Sarah Knox
3CCEFD32770D488...

Ophir Klein
Torsten Wittmann
Sarah Knox

Committee Members

Dedication

I am truly grateful for everyone who has supported and guided me to this point, and I dedicate this work to the individuals below.

To my parents, Hansil and Sooneeh, for their unconditional love and support and for believing in me when I had doubts in myself. I will always remember your love and sacrifice.

To my brother, Jaewha, for being someone that I can always reach out to chat when I am happy or down.

To Yoland for understanding the decision I have made and going through the journey together.

Acknowledgments

My journey at UCSF has been filled with precious memories and relationships that I will treasure forever. I have grown tremendously professionally and personally. As I take my next step into my career, I would like to acknowledge everyone who has filled this chapter of my life.

Thank you to my PhD thesis advisor and mentor, Ophir D Klein, MD, PhD, for believing in me, and supporting me with great care and patience. At every stumble I made along my journey, you have patiently guided me and encouraged me to get back on track. I feel very fortunate to have had you as my mentor. I am forever indebted to you for pushing me to strive for my best.

Thank you Jeremy BA Green, PhD, who has co-mentored me on my thesis project. You and Ophir guided me through my training, challenged me to think critically and encouraged me to push through.

Thank you to my qualifying exam and dissertation committee members: Jeffrey O Bush, PhD; Sarah Knox, PhD; and Torsten Wittmann, PhD, for offering their insight and support throughout my training.

Thank you to past and present members of the Klein and the Green Lab for your thoughtful insights, intellectual contributions and efforts. I would like to especially thank Pauline Marangoni, PhD; Tingsheng Yu, PhD; Jingjing Li, PhD; Amnon Sharir,

PhD; Jan Prochazka, PhD; Jimmy Hu, PhD; Adrian Joo, PhD; Asoka Rathnayake; Brooks Hoehn; Evelyn Sandoval.

Thank you Michel Bellini, PhD, my first research mentor while I was an undergraduate in University of Illinois at Urbana-Champaign. You have introduced me to research and taught me how rewarding and exciting research can be. You have inspired me to pursue this path.

Thank you to my clinical mentors at the UCSF School of Dentistry, Diana Nguyen, DDS; Samuel Chiu, DDS; Irene Cheng, DDS; Kimberly Morita, DDS; and Tamara Adams, DDS; Maungmaung Thaw, DDS; Wilson Hsin, DMD, for sharing your wisdom inside and outside of clinic, and encouraging me to become a better clinician.

Thank you to my amazing friends: Jerry Liu, DDS, MS; Goutam Krish, DDS; Katherine Le, DDS; William Lee, DDS; Julian Aurigui, Pharm D; Jarod Spohrer; Belle Lee; and Adrian Spanu; Joon Lee, DDS; Julian Huynh, DDS; Jungsoo Kim, DDS for all the shenanigans, emotional support and wonderful memories.

Thank you to Ralph Marcucio, PhD; Pamela Den Besten, DDS, MS; and Deans John Featherstone, PhD and Michael Reddy, DMD, DMSc for your dedication to the DDS/PhD dual training program and ensuring the trainees are receiving the best learning opportunity.

Thank you, Roger Mraz, for being an incredible program administrator for the dual training program and friend.

I am truly grateful for the relationships that I have built within and outside of UCSF. Every one of them has helped me grow. Without these individuals, I would not stand where I stand. It truly takes a village.

Contributions

Part of chapter 1 of this dissertation is adapted from the manuscript as it appears in Developmental Dynamics (2017). Chapter 2 of this dissertation is a revised version of the manuscript as it appears in Development (2021). The authors listed of the manuscript directed and/or contributed to the research that forms the basis for the thesis.

Kim R., Green J.B.A., Klein O.D. (2017) From snapshots to movies: Understanding early tooth development in four dimensions. Dev. Dyn. 2017;246:442–450.

Kim, R., Yu, T., Li, J., Prochazka, J., Sharir, A., Green, J. B. A. and Klein, O. D. (2021). Early perturbation of Wnt signaling reveals patterning and invagination-evagination control points in molar tooth development. Development 148.

Abstract

Early perturbation of Wnt signaling reveals patterning and invagination-evagination control points in molar tooth development

By

Rebecca Yewon Kim

The developing tooth offers a model for the study of ectodermal appendage organogenesis. The signaling networks that regulate tooth development have been intensively investigated, but how cell biological responses to signaling pathways regulate dental morphogenesis remains an open question. One of the challenges has been the lack of tools to study the role of the odontogenic signaling pathways in specific time and space. This dissertation investigates the role of Wnt/β-catenin pathway during the earliest stages of tooth development through utilizing a unique combination of genetic tools that the our has been previously identified.

Tooth formation involves an orchestration of different signaling pathways both within the oral epithelium and between the epithelium and the underlying mesenchyme. Previous studies of the Wnt/β-catenin pathway have shown that tooth formation is partly inhibited in loss-of-function mutants, and gain-of-function mutants have perturbed tooth morphology, such as hyper-calcification of existing dentition and formation of

supernumerary teeth. However, the stage at which Wnt signaling is first important in tooth formation has not been elucidated.

Our lab previously identified *Fgf8* as one of the earliest markers of tooth development in mouse. Building on this knowledge, I induced *Fgf8*-promoter-driven and therefore early deletion of β-catenin in molar epithelium and discovered that loss of Wnt/β-catenin signaling completely deletes the molar tooth, demonstrating that this pathway is central to the earliest stages of tooth formation. Early expression of a dominant-active β-catenin protein also perturbs tooth formation, producing a large domed evagination at early stages and supernumerary teeth later on. The early evaginations are associated with premature mesenchymal condensation marker, and are reduced by inhibition of condensation-associated collagen synthesis. This dissertation proposes that invagination versus evagination morphogenesis is regulated by the relative timing of epithelial versus mesenchymal cell convergence regulated by canonical Wnt signaling. Together, these studies reveal new aspects of Wnt/β-catenin signaling in tooth formation and epithelial morphogenesis more broadly.

Table of Contents

List of Figures

Chapter 1:

Introduction

Background

Ectodermal appendages, including the hair follicle, mammary gland, nail, and tooth, initiate development through a shared program that involves induction and placode formation (reviewed in Biggs and Mikkola, 2014). The murine tooth provides an excellent model system to investigate the development of these ectodermal organs, as it is relatively large and can be easily accessed and manipulated. Importantly, the signaling pathways that regulate tooth development are well conserved in different tooth types and between species, as well as during the development of related organs (Fraser et al., 2009; Tummers and Thesleff, 2009).

In mice, the first morphological sign of tooth development is observed at embryonic day (E) 11.5, with the appearance of localized thickenings of the oral epithelium known as dental placodes (Fig. 1.1; reviewed in Tucker and Sharpe, 2004). The instructive information for tooth development resides in the dental epithelium at this stage, and the epithelium has the potential to induce odontogenic fate in any neural crest-derived mesenchyme to form tooth (Mina and Kollar, 1987; Lumsden, 1988).

By the early bud stage (E12.5), the placode continues to stratify and invaginate to form the dental lamina, and underlying mesenchyme begins to condense. At this stage, the odontogenic potential shifts to the mesenchyme. *Pax9* and *Msx1* expression are hallmarks of the dental mesenchyme in the bud and are required for mesenchymal *Bmp4*

expression, which is important for progression through the subsequent odontogenic stages (Chen et al., 1996; Neubuser et al., 1997; Tucker et al., 1998). By E14.5, the tooth bud extends around the dental mesenchyme (also called the dental papilla) to form a cap-shaped epithelium also known as the enamel organ. A group of post-mitotic cells called the primary enamel knot that forms within the dental epithelium regulates tooth crown development at the cap stage. Signaling molecules secreted by the enamel knot, which include members of the Hh, Wnt, Bmp, and Fgf families, play a crucial role in shaping the tooth by maintaining the enamel knot and regulating cell proliferation in adjacent cells that is thought to drive the folding of the epithelium into cusps (Jernvall et al., 1994, 2000; Harjunmaa et al., 2014).

In addition, the enamel knot expresses markers such as *p21*, *Msx2*, and *Bmp2* to induce growth arrest and subsequently apoptosis of the signaling center (Vaahtokari et al., 1996; Aberg et al., 1997; Jernvall et al., 1998; Thesleff et al., 2001). At E15.5–17.5, the epithelium continues to invaginate, and concurrently, secondary enamel knots form at a distance from the disintegrating primary enamel knot and control the location and shape of the tooth cusps (Thesleff et al., 2001; Matalova et al., 2005). The shape and size of the tooth is determined throughout these stages, and thus, the early odontogenic stages are critical for determining adult dental morphology. During late odontogenic stages, dental epithelial and mesenchymal cells differentiate into ameloblasts and odontoblasts that lay down enamel and dentin, respectively. Other cell types, such as cementoblasts and cells of the periodontal ligament, differentiate at these stages as well.

The field has accumulated a wealth of knowledge regarding the molecular regulation of tooth development, but how individual dental epithelial and mesenchymal cells translate these molecular signals into an integrated morphological output remains unclear, especially during the earliest stages of tooth development. One constraint has been that, until recently, the molecular and genetic studies regarding tooth morphogenesis have been studied using static histological analyses in stages much later than the initial onset of the phenotype. While such an approach offers us clues about the cellular basis of morphogenesis, it limits our understanding of tissue behaviors, as we are limited to deducing highly dynamic, three-dimensional (3D) cellular activities from sequential, often 2D, snapshot analyses. For instance, rigorous histological analysis of the developing incisor placode led to the proposal that an early signaling center located within the incisor field is a rudimentary tooth that subsequently undergoes apoptosis and disintegrates (Hovorakova et al., 2011).

Recently, several groups have proposed different models for how a tooth germ develops using *ex vivo* imaging techniques on live tissue to link genetics and signaling with the physical morphogenesis of the tooth. Importantly, live explants faithfully recapitulate normal development in terms of tissue morphogenesis, and many gene expression and differentiation markers appear as normal.

1.1 Molar Signaling Centers

The textbook version of the signals governing molar tooth development is that the process is initiated and organized by a single signaling center, the initiation center or primary enamel knot precursor, in the middle of each placode. However, recently more detailed and dynamic analysis has revealed a more complicated picture. The fibroblast growth factor (Fgf), Sonic Hedgehog (Shh), Wnt, and BMP signaling pathways all play multiple roles throughout tooth development. In particular, *Fgf8* and *9*, are expressed in the dental placode, and *Fgf10* is expressed in the mesenchyme from the placode's earliest appearance. *Fgf8* expression appears even earlier in the entire proximal half of the jaw epithelium (Neubueser et al., 1997; Kettunen and Thesleff, 1998; Kettunen et al., 2000; Prochazka et al., 2015). *Fgf9*- or *Fgf10*-null mice form mineralized teeth with mild phenotypes, suggesting redundancy of FGF ligands (Yokohama-Tamaki et al., 2006; Haara et al., 2012). However, tissue-specific deletion of *Fgf8* arrested tooth development before the early bud stage, indicating that *Fgf8* cannot be compensated for by other Fgf family members during early tooth development (Prochazka et al., 2015).

It has been recently reported that the conventionally understood signaling center for the molar placode, as marked by expression of *Shh*, is at least transiently located more anterior to the molar placode itself, the latter being defined by cell movements, epithelial thickening, and enriched *Fgf8* expression. This was detected by genetic labeling of the *Shh*- and *Fgf8*-expressing populations in a mouse embryo using the double driver strain $Shh^{Egfp/Cre};Fgf8^{lacZ}$ (Prochazka et al., 2015). Surprisingly, the proximal *Fgf8* center also

expresses *Shh* target genes, despite not apparently expressing *Shh* itself. It still remains unclear at what points the *Fgf8*-expressing molar placode and the *Shh*-expressing signaling center are distinct and whether, somehow, these coalesce. One possible explanation is that highly dynamic *Shh* expression, which marks the signaling center, appears in transient succession of spots from anterior to posterior direction. The earliest formation of *Shh*-expressing signaling center would transiently appear in diastema located between incisor and *Fgf8*-labeled molar region. Subsequently, it will form within the *Fgf8*-labeled molar region, which would eventually develop into tooth germ. This would be interesting to investigate *via* analyzing the formation of signaling center in 4D. In addition, future experiments involving assessment of temporospatial expression patterns as well as conditional inactivation of the odontogenic pathway regulators will improve our understanding of the dynamic regulation of the signaling network in the molar placode.

1.2 Odontogenic Signaling Network

Over the years, the field has accumulated a significant knowledge of the complex intra-tissue and inter-tissue network of signaling pathways involved in tooth development. It has become apparent that some of the key signaling repertoire involved in development of various ectodermal organs is used in tooth development. FGF, SHH, BMP and Wnt pathways are critical in regulating the early stages of tooth development.

As noted earlier, a member of FGF family, *Fgf8*, serves as a marker for molar epithelial progenitor cells during the initiation stage of the tooth development. Other Fgf ligands,

such as FGF9, 10 and 17 are also expressed during the initiation stage of the tooth development. Multiple members of Fgf pathway are expressed in multiple tissue compartments, including the singling center, throughout the tooth development, highlighting the importance of the pathway (reviewed in Du et al., 2018). In addition, several negative feedback regulators of Fgf signaling are expressed in the developing tooth, and these are prime candidates for control of these processes (reviewed in Thisse and Thisse, 2005). The Sprouty (Spry) gene family has been shown to regulate Fgf signaling in odontogenesis, and loss of *Spry2* and *Spry4* both result in persistence of Fgf signaling during early tooth development (Klein et al., 2006). *Mkp3* is another negative feedback regulator that is expressed adjacent to the *Fgf8*-expressing domain in the developing limb, at the midbrain/ hindbrain boundary, and in the maxillary, mandibular, and frontonasal prominence (Klock and Herrmann, 2002). *Mkp3* mRNA is also detected in the oral cavity at E11.5; thus, it will be interesting to test if the *Mkp3* expression pattern complements *Fgf8* expression within the *Fgfr2*-expressing domain.

The dynamics of the Wnt signaling, another key signaling pathway during tooth development, has also been extensively studied. A suite of Wnt ligands exhibit localized expression in dental epithelium and mesenchyme throughout tooth development, as well as the reporters of the active Wnt pathway, such as TOP-Gal, Axin2 and BAT-Gal (Ahn et al., 2010; Liu et al., 2008; Lohi et al., 2010). Reduced Wnt signaling activity, *via* either global deletion of the members of the Wnt pathway or overexpression of Wnt inhibitors, result in arrested tooth development at different stages (Andl et al., 2002; Liu et al., 2008;

Sasaki et al., 2005). In contrast, overactivation of Wnt pathway through genetical stabilization of β-catenin or genetic deletion of APC has resulted in supernumerary teeth and hypercalcified dentition, respectively (Jarvinen et al., 2006; Wang et al., 2009; Liu et al., 2008). While it is evident that the Wnt pathway has crucial role in tooth development, it is hard to uncover more precise role of Wnt pathway on cellular level as these studies are done through perturbation of such critical pathway in wide range of time and space. It would be important to use tissue-specific drivers, such Msx1-CreER, to further elucidate the role of Wnt pathway in tooth development. In addition, there are many negative and positive regulators of the Wnt pathway that could merit further study as well.

Additional signaling pathways, such as EDA signaling, are involved in fine-tuning the tooth morphogenesis. While the loss of this pathway can lead to hypodontia in mice with low penetrance (17%; Pispa et al., 1999), loss of EDA results in reduced tooth size and cusp number. Consistent with this, human patients carrying mutation in one or more of core genes of EDA pathway exhibit comparable clinical features as seen in mice with loss of EDA signaling. Of note, hypodontia with incomplete penetrance and hypomophic molars are often seen in human patients (Clarke, 1987). Notably, re-introducing EDA signaling to tooth germ *ex vivo* rescued the number of cusps in mouse molar in dose-dependent manner, suggesting its developmental and evolutionary role in tooth patterning (Harjunmaa et al., 2014).

1.3 Molar Progenitor Cell Migration

A very early event in tooth development was studied by Prochazka et al., who proposed that directed cell migration of transiently *Fgf8*-expressing cells is involved in formation of the tooth germ (Fig. 1.2A,B). The authors discovered that the expression domain of *Fgf8* in the mandibular epithelium is predominantly in the proximal region of the mandible at E11.5, the placode stage of tooth development (Prochazka et al., 2015). Genetic lineage tracing together with ablation of this population revealed that *Fgf8*-expressing cells are progenitors that give rise to the entire molar epithelium and thus are required for progression through subsequent odontogenic stages.

Building on this knowledge, the authors used *Fgf8*-driven tamoxifen-dependent Cre recombinase to study the cellular dynamics in the molar placode at E11.5. They showed that, at E11.5, the dental epithelial progenitor cells at the proximal region adopt elongated shapes and arrange into a large (perhaps 100–200 mm diameter), rosette-like structure. Such anterior movement would bring these cells toward the above-mentioned *Shh*-expressing center. Analyses of cells labeled using $Fgf8^{ires\text{-}Cre}$ revealed that the cells within the rosette-like structure underwent more directed and dynamic cell migration, compared with cells that are located posteriorly to the rosette-like structure (Fig. 1.3A,B).

Genetic and pharmacological perturbation of the Fgf and Shh pathways resulted in deregulated migration of these dental epithelial cells. However, the two pathways may control different aspects of cell migration. Upon chemical inhibition of the Fgf pathway,

using a relatively low dose of the inhibitor SU5402, cell migration was no longer visible; whether this was due to arrest of migration as such, or to the non-formation of a migratory suprabasal layer of cells, remains an open question, as discussed below. Upon chemical inhibition of the Shh pathway, the placodal cells still moved in the general distal-ward direction of the future tooth germ but failed subsequently to converge toward the center of the future tooth. Interestingly, this low-dose pharmacological inhibition of either Fgf or Shh signaling had no apparent effects on cell proliferation and apoptosis. However, as discussed next, the role of these pathways is still somewhat unresolved.

Prochazka et al. also observed that genetically hyperactivating Shh signaling, using *Fgf8*^{CreER}*;R26R*^{SmoM2}, resulted in distal expansion of the tooth germ into the normally toothless diastema region that separates the incisor from the molars. It has been previously reported that two successive and transient bud-like structures in the diastema may be the rudimentary precursors of the premolars present in ancestral species (Prochazka et al., 2010). These rudimentary buds can develop into a supernumerary tooth in several mutants (Klein et al., 2006; Lochovska et al., 2015). It will be interesting to further investigate if the expanded tooth germ upon increased Shh activity can contribute to supernumerary tooth formation.

1.4 Molar Epithelial Stratification And Bending

A second study, by Li et al., demonstrates regulatory roles for the Fgf and Shh pathways in early tooth morphogenesis in addition to instructing epithelial cell migration (Li et al., 2016b). In this study, it was reported that chemical inhibition of the Fgf pathway in E11.5 mandibles significantly impaired the proliferation of the dental epithelial cells, resulting in failure of epithelial stratification of the molar tooth germ (Fig. 1.4B). However, inhibiting the Fgf pathway after E11.5, when some stratification had already occurred, arrested further proliferation but did not prevent invagination of the developing tooth germ (Fig. 1.4E).

In a complementary experiment, the authors ectopically activated the Fgf pathway by introducing FGF10-soaked beads to single-layered tongue epithelium. Exposure to recombinant FGF10 promoted the stratification of tongue epithelium, suggesting that Fgf signaling is both necessary and sufficient to induce epithelial stratification.

The effects of FGF inhibition on proliferation were thus different from those reported by Prochazka et al. One possible explanation for the discrepancies could be the different level of pharmacological treatment. Prochazka et al. exposed the whole mandible explant to 2.5 mM of Fgf pathway inhibitor (SU5402), whereas Li et al. treated mandibular tissue slice culture with 20 mM SU5402. Clearly, the higher dose applied to a smaller piece of tissue could have had different effects, although it was found still to be well below that needed to produce cell death (Li et al., 2016b). Several studies have shown that the Fgf

pathway can elicit differential cellular responses, including cell proliferation, migration, and differentiation, through activation of different downstream pathways (reviewed in Boilly et al., 2000). For instance, half maximal activity of cell migration required higher FGF concentrations compared with cell proliferation in rat lens epithelial explants (McAvoy and Chamberlain, 1989).

It is possible that the dosage used by Prochazka et al. was sufficient to perturb the cell migration, while having a negligible effect on cell proliferation. It is also possible that different durations of drug exposure could have led to different cellular responses, or that differences in experimental setup could explain the distinct outcomes. Further investigation of dose- and duration-dependent response of the dental placode cells to SU5402 through analyzing different downstream pathways would help resolve this discrepancy. Also, the role of Fgf signaling in the dental mesenchyme should be investigated, as Fgfr1IIIc is expressed in the dental mesenchyme at the earliest stages of tooth development (Kettunen and Thesleff, 1998). Reconciling the observations this way would also require that inhibition of the early migration not affect the later cell movements associated with deepening invagination. A recent study showed that the inhibitory effect of SU5402 may not be limited to Fgf signaling, but rather can extend to other tyrosine kinases, and differential dosage and duration of SU5402 treatment may also elicit distinct off-target effects (Gudernova et al., 2016). Therefore, more spe- cific suppression of Fgf signaling, perhaps through genetic dele- tion of Fgf receptors, may help to address this issue.

Of interest, the dental placode increased in width at the expense of the depth of invagination upon chemical inhibition of Shh signaling (Fig. 1.4D,G). The resulting shallower, wider invagination has also been observed in Shh and Hh pathway genetic hypomorphs and knockouts, not only in tooth but also in hair follicles, which are thought to be formed at these early stages by much the same signaling and morphogenetic processes (reviewed in St-Jacques et al., 1998; Gritli-Linde, 2002; Pispa and Thesleff, 2003; Prochazka et al., 2015). In the study by Li et al., hyperactivation of the pathway resulted in the opposite phenotype, with accelerated narrowing and deepening of the placode invagination. In both cases, careful quantification showed that there was no significant change in overall cell proliferation rate and apoptosis.

These results collectively indicate that the Shh pathway has a regulatory role in epithelial cell rearrangement. The Fgf and Shh pathways together may promote asymmetric cell proliferation that leads to local epithelial stratification and regulation of cell tension and/or motility that leads to epithelial bending. The authors suggest that these processes jointly drive the invagination of the molar epithelium into the underlying mesenchyme.

The study by Li et al. demonstrated that Fgf and Shh signaling can promote cell proliferation and epithelial bending, respectively, through gain- and loss-of-function approaches. One important point that could be followed up in the future is that the experimental framework used in the gain-of-function experiments exposed the entire explant to chemical Shh agonist. The lack of a restricted or graded spatial distribution of

signal and the degree of signaling activity that may be outside the physiological range may have led to cells not responding in a physiological manner, although a similar effect was seen with SHH protein applied by means of a protein-soaked bead (Cobourne et al., 2004). It is also worth noting that the experiments could not distinguish between roles of the Shh signal in orienting cell migration versus triggering or maintaining migration as such. Because expression of *Shh* in the tooth germ is spatially separated from the early molar placode and localized to the distal tip of the early tooth bud, it is even possible that tissue slices, which would normally successfully have undergone invagination, did not contain the endogenous source of *Shh* (Prochazka et al., 2015). Verifying the endogenous *Shh* expression within the tissue slice culture would strengthen the relationship between the experimental observations and events that occur in vivo.

1.5 Suprabasal Cell Intercalation-Mediated Contraction

One possible cellular mechanism through which Shh signaling promotes epithelial bending is through interaction of cells in the suprabasal layer, as demonstrated by the Li et al. study described above and another from the same group (Panousopoulou and Green, 2016). Using the molar placode as a model, these authors showed that invagination of the placode is driven by *Shh*-dependent horizontal intercalation of suprabasal cells (Fig. 1.2C,D). These suprabasal layers of cells in the tooth germ form a shrinking and thickening canopy over underlying epithelial cells. Experimental incision through the epithelium and mesenchyme that flank the molar placode in jaw slice explants resulted in elastic recoil from the incision site (Fig. 1.5A). When the incision was

introduced specifically in the suprabasal layer, but not the basal layer, the suprabasal layer recoiled laterally from the cut. When an initial incision through the suprabasal cell layer was followed by lateral incision of the flanking tissues, this essentially abolished the recoil of the molar placode (Fig. 1.5B). These data suggest that the suprabasal cells, but not the basal cell layers, generate a tensile force sufficient and necessary to invaginate the molar placode. The intercalating tissue is, critically, anchored at its edges to the basal lamina by shoulder cells that both contact the lamina basally and intercalate apically. Crucially, Hedgehog pathway inhibition arrested the suprabasal canopy contraction and abolished the intercalation-associated planar cell elongation in both supra- basal and shoulder cells (Li et al., 2016b).

Given that the above experiments were done in slice explants, effects of the inhibition on long-range planar migration, of the kind observed by Prochazka et al., could not be tested. As with the Fgf inhibition, there might seem to be a discrepancy between the two sets of Shh inhibition experiments. The Prochazka et al. work showed little effect of Hedgehog pathway inhibition on cell motility as such, and the Li et al. treatments in effect arrested cell movement. However, in the both cases, there was a definite inhibition of cell convergence, and this may indicate that the Shh signal provides a directional cue rather than a migratory signal as such, and that the later intercalation of cells in the invaginated tooth bud may be more sensitive to its absence than the earlier superficial migration. It would be interesting to see how Shh signaling inhibition affects cell movement and intercalation in real time using time-lapse confocal imaging on pharmacologically treated

tissue. Further insights into the cellular response to Shh may be needed, because *Gli1* expression is widespread in the tooth and gives few clues as to how it might provide directionality.

Panousopoulou and Green observed enriched actomyosin com- plex and E-cadherin punctae at the surfaces of the suprabasal cells. They proposed that E-cadherin-based spot adherens junctions enable the cell intercalation, which in turn pulls the tissue toward the midline to hold its morphology. The authors suggested that this process also seals the top of the tooth germ so that cell proliferation and delamination below the intercalating layer further forces the underlying epithelial cells to invaginate into the mesenchyme. The intercalating suprabasal cells are replenished, in part by the incorporation of delaminating basal cells.

The authors 3D-rendered the nuclear morphology in the molar placode, using deformation from a spherical shape to reveal the external forces experienced by the cells. They showed that the tension in the suprabasal layer stretched the nuclei from the default sphere shape of unstressed cells into a flattened “lentil” shape, indicating the equal magnitude of force exerted in all directions in the epithelial plane. It is apparent that the cells experience a tensile force along the lingual–buccal axis that results in the most commonly depicted epithelial invagination, but that a similar force in the proximodistal axes of the jaws sustains invagination in that aspect to form the front and rear of the elongated pit or “boat” shape of the early molar tooth. It will be interesting to further assess

which cell behaviors contribute to this proximodistal force.

1.6 Cell Behaviors Along Different Axes

The Prochazka et al. and the Panousopoulou et al. experiments describe two quite seemingly different cell migrations. One involves distal migration of cells distally from the jaw hinge while the other is a convergence of cells into the invaginating tooth bud. One is apparently FGF-dependent, the other FGF- independent. One is apparently Hedgehog pathway oriented, the other, Hh pathway dependent, which bags the following question: How can these discrepancies be accounted for? One possible explanation involves the different explant culture techniques used to image the tissue. The directed cell migration events proposed by Prochazka et al. are supported by live-tissue imaging of E11.5 hemi-mandible using spinning disk confocal microscopy. The entire hemi-mandible was imaged *en face* from the oral surface, and the images obtained were processed by maximal intensity projection for cell tracking analysis. This computational method projects the 3D information into two dimensions, and the subsequent analysis does not focus on the tracking information along the rostral–caudal axis.

In contrast, Panousopoulou and Green's suprabasal cell intercalation hypothesis is based on imaging of tooth slices. This method allows observation of the cell behavior that occurs along the vertical (superficial-to-deep) axis without compromising the resolution. However, the tissue slice preparation would likely remove more proximal tissue. Because Prochazka et al. propose that cell migration toward the *Shh*-signaling center comes from

more proximal tissue, this would be largely or entirely absent in the slice cultures. The successful invagination of the placode, which apparently occurs normally in slice cultures, despite the likely absent proximal tissue (near the jaw hinge), suggests that the cell migration and cell intercalation are independent events. It is even possible that slice culture removes critical distal signals or perturbs proximodistal signals in other ways.

Another possibility is that the two events take place in a sequential manner: the dental epithelial cells first migrate distally and define the position and the size of the future tooth germ along the proximodistal axis, and then they start to proliferate and intercalate to grow and invaginate into the underlying mesenchyme. Various factors can influence the developmental schedule of embryogenesis (e.g., genetic background, transgenic and mutant alleles, and tamoxifen administration) (Dandekar and Glass, 1987; Naiche and Papaioannou, 2007). Therefore, it is possible that the staging of embryos in the two studies were slightly different. One conceptually simple experiment to test this would be to perform live imaging on intact jaw explants (i.e., not slices) in a single genetic background using multiphoton microscopy, which may allow for greater imaging depth compared with traditional spinning disk confocal microscopy, and then analyzing the cell behaviors in four-dimensions.

1.7 Signaling Centers in Early Incisor Development

Many signaling cascades, including the Shh and Fgf pathways, are iteratively activated in both the incisor and the molar placodes. A recent study by Ahtiainen et al. performed

ex vivo analysis of the developing incisor placode in a fluorescent ubiquitination-based cell cycle indicator (Fucci) mouse to understand the molecular regulation of cell behaviors in the incisor placode (Ahtiainen et al., 2016). The authors demonstrate that there is a population of nonmitotic cells that resides in the incisor placode near the oral surface. Time-lapse confocal imaging reveals that while these cells actively migrate toward the midline of the tooth bud to condense, the total number of cells remains relatively constant. Once condensed, these cells may act as a signaling center to regulate the early stages of incisor development (Fig. 1.2E), as the location of the nonmitotic cells coincides with the expression of signaling molecules that regulate tooth development.

The authors define this early population of quiescent, morphogen-secreting cells as the "initiation knot." Cell quiescence is a common feature of signaling centers in various organs, including the apical ectodermal ridge of the developing limb bud, the developing hair placode, and the enamel knot in the developing tooth germ (Jernvall et al., 1994; Martin, 1998; Ahtiainen et al., 2014). Notably, the authors reported that the initiation knot, which appears very early, and the enamel knot, which appears later during odontogenesis, are distinct cell populations. Tracking individual cells in the initiation knot of the mandibular explant revealed that these cells remained within clear boundaries near the oral surface, whereas the enamel knot appeared *de novo* at the tip of the mature bud (Fig. 1.1F). This observation is consistent with a previous study that demonstrated, using finely staged embryos, that the two spatially distinct signaling centers appear sequentially (Hovorakova et al., 2011, 2013).

While the cells in the initiation knot remain quiescent, the may promote proliferation in the neighboring cells to drive tooth morphogenesis. To test this possibility, the authors use *Tabby* mice, which exhibit smaller tooth and cusp patterning defect due to mutations in the Eda/Edar/NF-kB pathway (Pispa et al., 1999; Harjunmaa et al., 2014). The authors found that the overall number of quiescent cells and the volume of the initiation knot were reduced in *Tabby* mice. In turn, the smaller initiation knot resulted in reduced expression of genes that are important for progression of tooth development, suggesting a link between the size of the initiation knot and that of the resulting tooth bud.

One alternative explanation would be that the smaller initiation knot and tooth bud are independently initiated but sequential events. While it is likely that the tooth bud depends on specific molecular signals from the initiation knot, it could also be that the Eda/Edar/NF-kB pathway determines the size of the dental anlage, and the smaller initiation knot would be a secondary result of a hypomorphic tooth germ. One way to address this would be to perform spatiotemporal ablation of the initiation knot cells. Another remaining question is whether the smaller tooth germ in *Tabby* mice results from reduced mitogenic signal in the initiation knot. This can be addressed in the future by unbi- ased molecular characterization of the initiation knot and quantitative analysis of cell proliferation in the tooth germ of *Tabby* mice.

1.8 Cell Behaviors in Molar vs. Incisor Epithelium

Cell migration has been observed in various morphogenetic contexts (reviewed in Aman and Piotrowski, 2010). As described above, molar placode cells migrate and this is essential for forma- tion of the tooth germ; however, in the incisor, as observed by Ahtiainen et al., the migration seems to be limited to the cells in the initiation knot, whereas cell proliferation seems to be the main driving force for subsequent invagination. One possible reason for this discrepancy is the difference in the developmental timing of incisor and molar. Ahtiainen et al. studied similar embryonic stages (E11.5 and E12.0) to those in the molar-focused papers reviewed above.

However, because development of the incisor is faster than that of molar, it is likely that Ahtiainen et al. analyzed the cell behav- iors at more advanced stages of tooth development. Later stages in molar morphogenesis were not analyzed by either Prochazka et al. or the Green group, and it would be interesting to see if later stages of invagination are, like the incisor, dominated more by proliferation processes than by cell movement. Conversely, an examination of incisor at earlier stages and at higher resolution might reveal similarities to the molar, because Ahtiainen et al. made their observations at relatively low magnification.

Another possibility is that signaling centers in incisors and molars have qualitatively different instructive roles. It is important to note that the molar signaling center is spatially distinct from the molar placode, whereas the incisor signaling center (*i.e.*, initiation knot) is located within the incisor field. Moreover, morphogenesis of the incisor and the molar

placode differ on a 3D level. The incisor placode maintains its location and adopts a relatively rounder shape as it develops, whereas the molar placode undergoes significant expansion along the proximodistal axis to adopt its cylindrical shape. Therefore, it is conceivable that cells respond differently to the same signals to contribute to the morphogenesis of the two tooth types.

1.9 Conclusions and Future Prospects

The studies discussed in this review have enhanced our under- standing of how molecular signaling translates into dental epithelial cell dynamics. However, many mysteries remain, and it is certain that tooth morphogenesis is more complex than our cur- rent understanding. Most studies of tooth development have focused on the epithelial contribution due to the availability of genetic tools and the tissue's well-defined structure. However, it is well known that epithelium and mesenchyme exchange highly dynamic and reciprocal signaling to orchestrate tooth development. The dental mesenchyme takes on an instructive role between E11.5 and E12.5, during which placodal invagination occurs, suggesting that mesenchymal signaling is critical for directing epithelial invagination (Mina and Kollar, 1987).

Panousopoulou and Green showed by explantation that the initial invagination forces in the molar were autonomous to the epithelium, but it is theoretically possible that the dental mesenchyme coordinately undergoes remodeling to facilitate invasion by the invaginating epithelium (Panousopoulou and Green, 2016). The presence of abundant F-actin and

phosphomyosin in jaw mesenchyme also allows for the possibility of a role of mesenchyme during tooth development. Therefore, investigating dental mesenchymal dynamics would be a logical next step to further our understanding of tooth morphogenesis. Recently, tamoxifen-inducible Cre lines under control of promoters of early dental mesenchymal markers, such as *Fgf10* and *Msx1*, have been generated, and these may be useful for future studies (El Agha et al., 2012; Lallemand et al., 2013). In parallel, the field has also begun to explore dental mesenchymal cell dynamics through combining ex vivo imaging with tissue recombination techniques (Mammoto et al., 2011; Li et al., 2016a).

In addition, there are several exciting studies that investigate cellular behaviors underlying different processes of tooth morphogenesis which have not been highlighted in this review. While this review focuses on dental placodal invagination, it is equally interesting to understand the process through which placodes are formed. Li et al. suggest that the vertical mitotic angle of placodal cells relative to the basement membrane may promote the thickening, suggesting that perturbation of genes known to be involved in regulating mitotic orientation could further this line of investigation (Li et al., 2016b). Another group explored the mechanism through which bud-to-cap transition occurs. The tooth germ at E12.5, which is essentially an invaginated bud of epithelium, deforms into a distinct shape that resembles a cap by E14.5 (Fig. 1.1). To understand this process, Morita et al. combined long-term live imaging with Fucci cell cycle analysis, correlating the tissue growth pattern with mitotic orientation and frequency in the tooth germ at E14.5 (Morita

et al., 2016). The authors reinforced previous studies showing that differential cell proliferation is one of the driving forces of tooth morphogenesis (Jernvall et al., 1994). In addition, through quantitative analysis of fluorescence recovery of YFP-actin after photobleaching, the authors showed that dynamic actin remodeling might play a role in tooth germ morphogenesis.

Another interesting question is the mechanism through which the second and third molars develop. Both humans and mice develop three molars per jaw quadrant, with each subsequent molar forming at the posterior of the previous tooth germ. Gaete et al. explored this phenomenon at tissue and cellular level. Through combining explant culture with DiI labeling and tissue truncation, they found that second and third molars are derived from progenitors that reside in the "tail" of the first molar tooth germ, a structure more superficial than the bulk of the tooth germ (Gaete et al., 2015). This finding complements previous work examining development of molars (Juuri et al., 2013). Investigating different stages of tooth morphogenesis will provide us with an understanding of how the dental organ derives its characteristic 3D shape from a flat epithelial sheet.

The tooth has long been an important model for developmental biologists. A deeper understanding of the morphogenetic events in tooth development will be of broad significance to the field of organogenesis, as many signaling pathways and cellular events in tooth development are not restricted to odontogenesis, but rather are deployed in various developmental contexts.

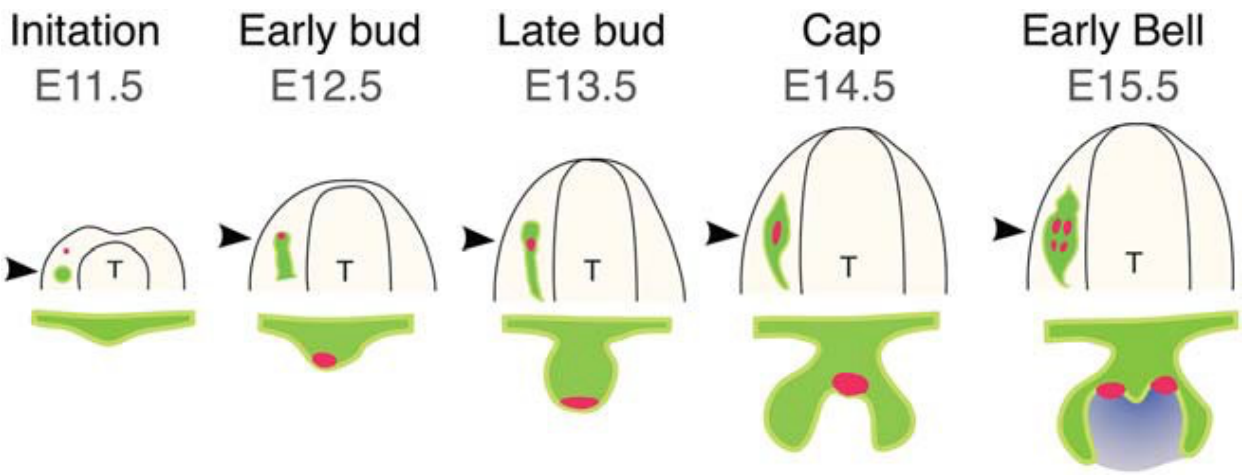

Figure 1.1. Early stages of molar development. The first morphological sign of molar development is observed at E11.5, with the localized thickening of the oral epithelium to form dental placode. The placode continues to invaginate and grow into distinct 3D shapes during subsequent stages. The shape and size of the tooth is determined through- out these stages, and thus, the early odontogenic stages are critical for determining the adult dental morphology. Each stage is regulated by molecular cues from the signaling center. Top row illustrates the oral surface view of the whole mandible at respective embryonic (E) days. Bottom row illustrates frontal sections of the tooth germ at the locations indicated by arrowheads. T: tongue. Green: dental epithelium. Purple: dental papilla. Red: signaling center.

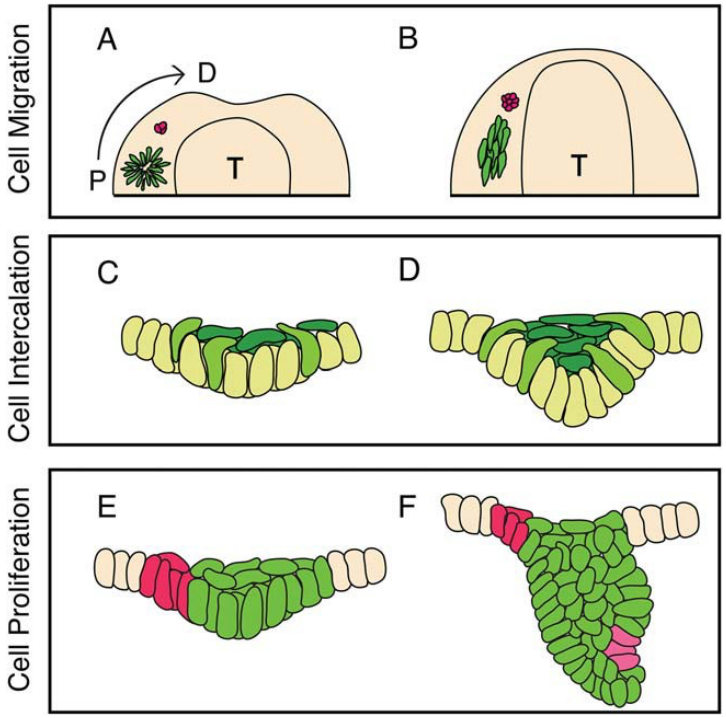

Figure 1.2. Cell movements in early tooth development. A,B: Prochazka et al. proposed that, viewing the mandible from above, progenitor cells in the molar placode (green) arrange into a rosette-like structure, then subsequently dissociate to migrate toward a *Shh*-expressing signaling center (red). C,D: In the model developed by Panousopoulou and Green, shown in frontal aspect, basal cells in the molar placode delaminate toward the center of the placode (yellow-green). The delaminated cells form the suprabasal tissue canopy (dark green), which intercalate along the midline to drive epithelial invagination. E,F: Ahtiainen et al. proposed that, in incisors, a population of nonproliferating cells that colocalizes with morphogen expression (red) instructs the neighboring epithelial cells (green) to proliferate, and this leads to tooth morphogen- esis. The enamel knot forms de novo at the tip of the tooth germ (pink). T: tongue. A and C are E11.5. B and D are E12.5. E is E12.0. F is E13.5.

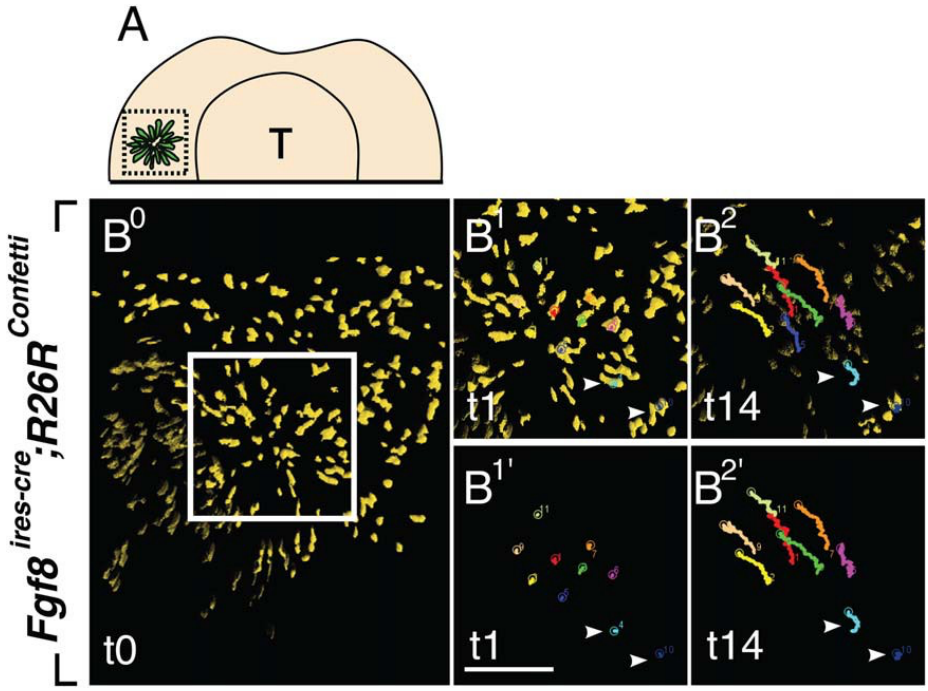

Figure 1.3. Fgf and Shh signaling instruct molar placodal cells to undergo directed cell migration. A: Schematic presentation of *Fgf8*-expressing molar placodal cells from oral surface view at E11.5. Dotted square demarcates the molar placode region. B–B$^{2'}$: Time-lapse imaging by means of spinning disk confocal microscopy reveals that *Fgf8*-expressing cells within the rosette-like structure are released and migrate distally. Tracking of the cells within the rosette-like structure (white box) over time (B^{1}–B^{2} and B$^{1'}$–B$^{2'}$). Arrowheads (lower right) indicate posterior cells that do not undergo dynamic migration. Scale bar: 100mm. Reproduced with permission from Elsevier.

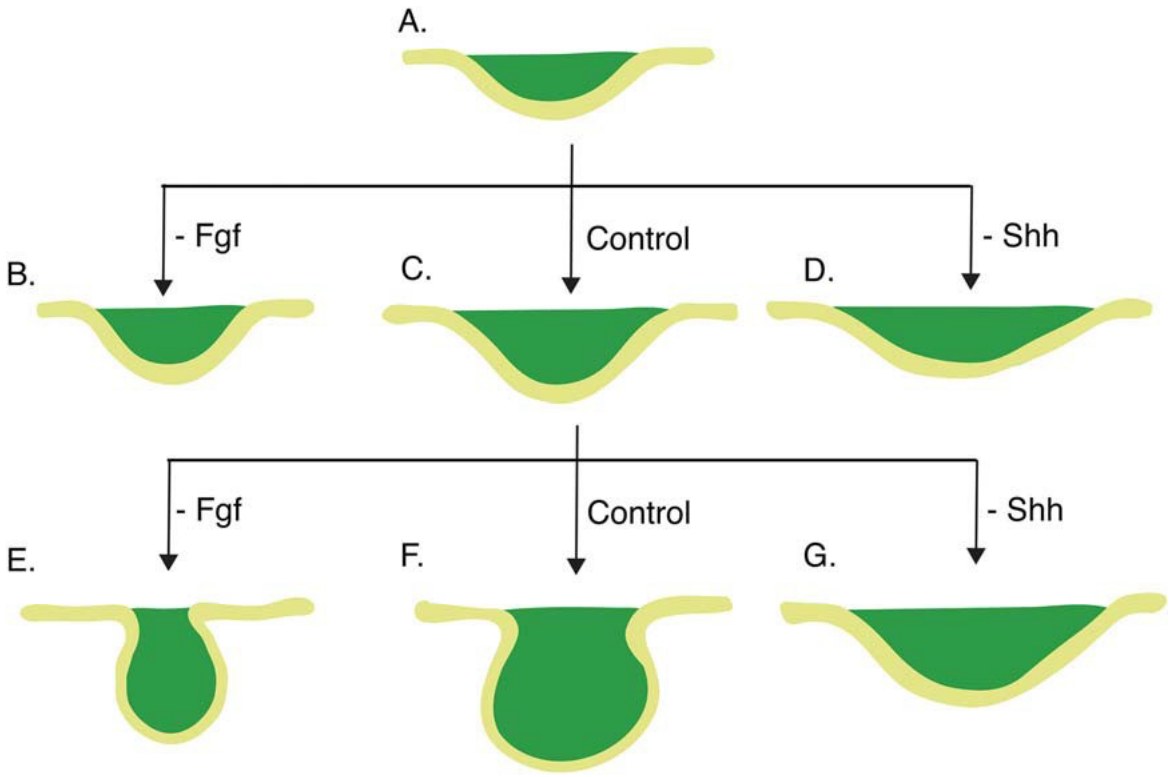

Figure 1.4. Fgf and Shh signaling promote stratification and epithelial bending, respectively. A–D: The molar placode (A) at E11.5 stratifies and bends into early tooth bud (C). However, inhibition of Fgf signaling results in significantly shallower tooth bud (B). Inhibiting the Shh pathway results in a shallower and wider tooth bud (D). E–G: Similar observation is made when the early tooth bud (C, E12.5) is treated with Shh and Fgf inhibitors. Early tooth bud further stratifies and invaginates into late tooth bud (F). However, inhibition of Fgf results in narrower tooth germ (G), while inhibit- ing Shh results in shallower and wider tooth germ (E). A: E11.5. B–D: E12.5. E–G: E13.5.

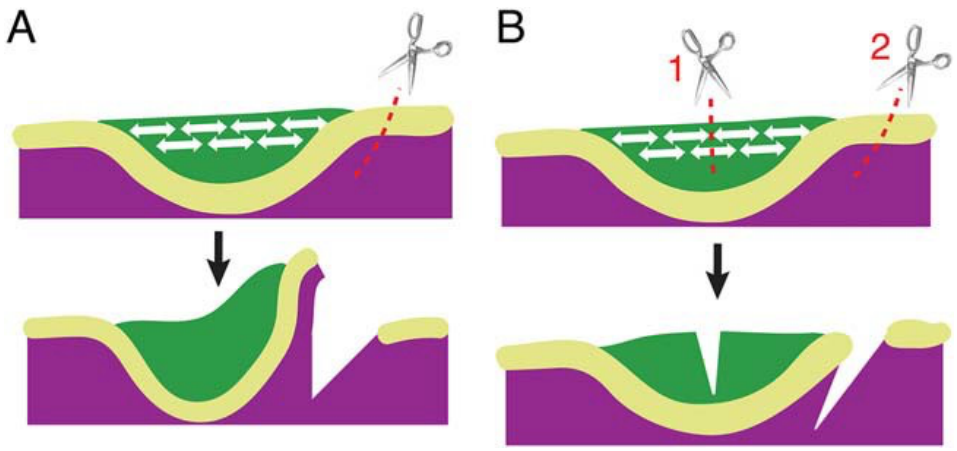

Figure 1.5. Contractile suprabasal tissue promotes bending of molar placode. A: Single lateral incision in the epithelium that flanks the molar placode at E11.5 allows rapid bending of the molar placode. B: Incision through the suprabasal layer (cut 1) abolishes the lateral cut- (cut 2) induced bending, showing that bending depends on suprabasal tension. Green: suprabasal layer. Yellow-green: basal layer. Purple: mesenchyme.

1.10 References

Aberg, T., Wozney, J. and Thesleff, I. (1997). Expression patterns of bone morphogenetic proteins (Bmps) in the developing mouse tooth suggest roles in morphogenesis and cell differentiation. *Dev Dyn* **210**, 383-396.

Ahn, Y., Sanderson, B. W., Klein, O. D. and Krumlauf, R. (2010). Inhibition of Wnt signaling by Wise (Sostdc1) and negative feedback from Shh controls tooth number and patterning. *Development* **137**, 3221-3231.

Ahtiainen, L., Lefebvre, S., Lindfors, P. H., Renvoise, E., Shirokova, V., Vartiainen, M. K., Thesleff, I. and Mikkola, M. L. (2014). Directional cell migration, but not proliferation, drives hair placode morphogenesis. *Dev Cell* **28**, 588-602.

Ahtiainen, L., Uski, I., Thesleff, I. and Mikkola, M. L. (2016). Early epithelial signaling center governs tooth budding morphogenesis. *The Journal of Cell Biology* **214**, 753-767.

Aman, A. and Piotrowski, T. (2010). Cell migration during morphogenesis. *Developmental Biology* **341**, 20-33.

Andl, T., Reddy, S. T., Gaddapara, T. and Millar, S. E. (2002). WNT signals are required for the initiation of hair follicle development. *Dev Cell* **2**, 643-653.

Biggs, L. C. and Mikkola, M. L. (2014). Early inductive events in ectodermal appendage morphogenesis. *Seminars in Cell & Developmental Biology* **25–26**, 11-21.

Boilly, B., Vercoutter-Edouart, A. S., Hondermarck, H., Nurcombe, V. and Le Bourhis, X. (2000). FGF signals for cell proliferation and migration through different pathways. *Cytokine & Growth Factor Reviews* **11**, 295-302.

Chen, Y., Bei, M., Woo, I., Satokata, I. and Maas, R. (1996). Msx1 controls inductive signaling in mammalian tooth morphogenesis. *Development* **122**, 3035-3044.

Clarke, A. (1987). Hypohidrotic ectodermal dysplasia. *J Med Genet* **24**, 659-663.

Cobourne, M. T., Miletich, I. and Sharpe, P. T. (2004). Restriction of sonic hedgehog signalling during early tooth development. *Development* **131**, 2875-2885.

Dandekar, P. V. and Glass, R. H. (1987). Development of mouse embryos in vitro is affected by strain and culture medium. *Gamete Res* **17**, 279-285.

Du, W., Du, W. and Yu, H. (2018). The Role of Fibroblast Growth Factors in Tooth Development and Incisor Renewal. *Stem Cells Int* **2018**, 7549160.

El Agha, E., Al Alam, D., Carraro, G., MacKenzie, B., Goth, K., De Langhe, S. P., Voswinckel, R., Hajihosseini, M. K., Rehan, V. K. and Bellusci, S. (2012). Characterization of a novel fibroblast growth factor 10 (Fgf10) knock-in mouse line to target mesenchymal progenitors during embryonic development. *PLoS One* **7**, e38452.

Fraser, G. J., Hulsey, C. D., Bloomquist, R. F., Uyesugi, K., Manley, N. R. and Streelman, J. T. (2009). An Ancient Gene Network Is Co-opted for Teeth on Old and New Jaws. *Plos Biology* **7**, 233-247.

Gaete, M., Fons, J. M., Popa, E. M., Chatzeli, L. and Tucker, A. S. (2015). Epithelial topography for repetitive tooth formation. *Biol Open* **4**, 1625-1634.

Gritli-Linde, A. B., M; Maas, R; Zhang, XM; Linde, A; McMahon AP (2002). Shh signaling within the dental epithelium is necessary for cell proliferation, growth and polarization. *Development* **129**, 5323-5337.

Gudernova, I., Vesela, I., Balek, L., Buchtova, M., Dosedelova, H., Kunova, M., Pivnicka, J., Jelinkova, I., Roubalova, L., Kozubik, A., et al. (2016). Multikinase activity of fibroblast growth factor receptor (FGFR) inhibitors SU5402, PD173074, AZD1480, AZD4547 and BGJ398 compromises the use of small chemicals targeting FGFR catalytic activity for therapy of short-stature syndromes. *Hum Mol Genet* **25**, 9-23.

Haara, O., Harjunmaa, E., Lindfors, P. H., Huh, S. H., Fliniaux, I., Aberg, T., Jernvall, J., Ornitz, D. M., Mikkola, M. L. and Thesleff, I. (2012). Ectodysplasin regulates activator-inhibitor balance in murine tooth development through Fgf20 signaling. *Development* **139**, 3189-3199.

Harjunmaa, E., Seidel, K., Hakkinen, T., Renvoise, E., Corfe, I. J., Kallonen, A., Zhang, Z. Q., Evans, A. R., Mikkola, M. L., Salazar-Ciudad, I., et al. (2014). Replaying evolutionary transitions from the dental fossil record. *Nature* **512**, 44-48.

Hovorakova, M., Prochazka, J., Lesot, H., Smrckova, L., Churava, S., Boran, T., Kozmik, Z., Klein, O., Peterkova, R. and Peterka, M. (2011). Shh expression in a rudimentary tooth offers new insights into development of the mouse incisor. *Journal of Experimental Zoology Part B: Molecular and Developmental Evolution* **316B**, 347-358.

Jernvall, J., Aberg, T., Kettunen, P., Keranen, S. and Thesleff, I. (1998). The life history of an embryonic signaling center: BMP-4 induces p21 and is associated with apoptosis in the mouse tooth enamel knot. *Development* **125**, 161-169.

Jernvall, J., Keranen, S. V. and Thesleff, I. (2000). Evolutionary modification of development in mammalian teeth: quantifying gene expression patterns and topography. *Proc Natl Acad Sci U S A* **97**, 14444-14448.

Jernvall, J., Kettunen, P., Karavanova, I., Martin, L. B. and Thesleff, I. (1994). Evidence for the Role of the Enamel Knot as a Control Center in Mammalian Tooth Cusp Formation - Nondividing Cells Express Growth-Stimulating Fgf-4 Gene. *International Journal of Developmental Biology* **38**, 463-469.

Juuri, E., Jussila, M., Seidel, K., Holmes, S., Wu, P., Richman, J., Heikinheimo, K., Chuong, C. M., Arnold, K., Hochedlinger, K., et al. (2013). Sox2 marks epithelial competence to generate teeth in mammals and reptiles. *Development* **140**, 1424-1432.

Kettunen, P., Karavanova, I. and Thesleff, I. (1998). Responsiveness of developing dental tissues to fibroblast growth factors: expression of splicing alternatives of FGFR1, -2, -3, and of FGFR4; and stimulation of cell proliferation by FGF-2, -4, -8, and -9. *Dev Genet* **22**, 374-385.

Kettunen, P., Laurikkala, J., Itaranta, P., Vainio, S., Itoh, N. and Thesleff, I. (2000). Associations of FGF-3 and FGF-10 with signaling networks regulating tooth morphogenesis. *Dev Dyn* **219**, 322-332.

Klein, O. D., Minowada, G., Peterkova, R., Kangas, A., Yu, B. D., Lesot, H., Peterka, M., Jernvall, J. and Martin, G. R. (2006). Sprouty genes control diastema tooth development via bidirectional antagonism of epithelial-mesenchymal FGF signaling. *Dev Cell* **11**, 181-190.

Klock, A. and Herrmann, B. G. (2002). Cloning and expression of the mouse dual-specificity mitogen-activated protein (MAP) kinase phosphatase Mkp3 during mouse embryogenesis. *Mechanisms of Development* **116**, 243-247.

Lallemand, Y., Moreau, J., Clement, C. S., Vives, F. L. and Robert, B. (2013). Generation and characterization of a tamoxifen inducible Msx1(CreERT2) knock-in allele. *Genesis* **51**, 110-119.

Li, C. Y., Hu, J., Lu, H., Lan, J., Du, W., Galicia, N. and Klein, O. D. (2016a). alphaE-catenin inhibits YAP/TAZ activity to regulate signalling centre formation during tooth development. *Nat Commun* **7**, 12133.

Li, J., Chatzeli, L., Panousopoulou, E., Tucker, A. S. and Green, J. B. A. (2016b). Epithelial stratification and placode invagination are separable functions in early morphogenesis of the molar tooth. *Development*.

Liu, F., Chu, E. Y., Watt, B., Zhang, Y., Gallant, N. M., Andl, T., Yang, S. H., Lu, M. M., Piccolo, S., Schmidt-Ullrich, R., et al. (2008). Wnt/beta-catenin signaling directs multiple stages of tooth morphogenesis. *Dev Biol* **313**, 210-224.

Lochovska, K., Peterkova, R., Pavlikova, Z. and Hovorakova, M. (2015). Sprouty gene dosage influences temporal-spatial dynamics of primary enamel knot formation. *BMC Dev Biol* **15**, 21.

Lohi, M., Tucker, A. S. and Sharpe, P. T. (2010). Expression of Axin2 indicates a role for canonical Wnt signaling in development of the crown and root during pre- and postnatal tooth development. *Dev Dyn* **239**, 160-167.

Lumsden, A. G. (1988). Spatial organization of the epithelium and the role of neural crest cells in the initiation of the mammalian tooth germ. *Development* **103 Suppl**, 155-169.

Mammoto, T., Mammoto, A., Torisawa, Y. S., Tat, T., Gibbs, A., Derda, R., Mannix, R., de Bruijn, M., Yung, C. W., Huh, D., et al. (2011). Mechanochemical control of mesenchymal condensation and embryonic tooth organ formation. *Dev Cell* **21**, 758-769.

Martin, G. R. (1998). The roles of FGFs in the early development of vertebrate limbs. *Genes & Development* **12**, 1571-1586.

Matalova, E., Antonarakis, G. S., Sharpe, P. T. and Tucker, A. S. (2005). Cell lineage of primary and secondary enamel knots. *Dev Dyn* **233**, 754-759.

McAvoy, J. W. and Chamberlain, C. G. (1989). Fibroblast growth factor (FGF) induces different responses in lens epithelial cells depending on its concentration. *Development* **107**, 221-228.

Mina, M. and Kollar, E. J. (1987). The induction of odontogenesis in non-dental mesenchyme combined with early murine mandibular arch epithelium. *Arch Oral Biol* **32**, 123-127.

Morita, R., Kihira, M., Nakatsu, Y., Nomoto, Y., Ogawa, M., Ohashi, K., Mizuno, K., Tachikawa, T., Ishimoto, Y., Morishita, Y., et al. (2016). Coordination of Cellular Dynamics Contributes to Tooth Epithelium Deformations. *PLoS One* **11**, e0161336.

Naiche, L. A. and Papaioannou, V. E. (2007). Cre activity causes widespread apoptosis and lethal anemia during embryonic development. *Genesis* **45**, 768-775.

Neubüser, A., Peters, H., Balling, R. and Martin, G. R. (1997). Antagonistic Interactions between FGF and BMP Signaling Pathways: A Mechanism for Positioning the Sites of Tooth Formation. *Cell* **90**, 247-255.

Panousopoulou, E. and Green, J. B. (2016). Invagination of Ectodermal Placodes Is Driven by Cell Intercalation-Mediated Contraction of the Suprabasal Tissue Canopy. *PLoS Biol* **14**, e1002405.

Pispa, J., Jung, H. S., Jernvall, J., Kettunen, P., Mustonen, T., Tabata, M. J., Kere, J. and Thesleff, I. (1999). Cusp patterning defect in Tabby mouse teeth and its partial rescue by FGF. *Dev Biol* **216**, 521-534.

Pispa, J. and Thesleff, I. (2003). Mechanisms of ectodermal organogenesis. *Developmental Biology* **262**, 195-205.

Prochazka, J., Pantalacci, S., Churava, S., Rothova, M., Lambert, A., Lesot, H., Klein, O., Peterka, M., Laudet, V. and Peterkova, R. (2010). Patterning by heritage in mouse molar row development. *Proc Natl Acad Sci U S A* **107**, 15497-15502.

Prochazka, J., Prochazkova, M., Du, W., Spoutil, F., Tureckova, J., Hoch, R., Shimogori, T., Sedlacek, R., Rubenstein, J. L., Wittmann, T., et al. (2015). Migration of Founder Epithelial Cells Drives Proper Molar Tooth Positioning and Morphogenesis. *Dev Cell* **35**, 713-724.

Roehl, H. and Nüsslein-Volhard, C. (2001). Zebrafish pea3 and erm are general targets of FGF8 signaling. *Current Biology* **11**, 503-507.

Sasaki, T., Ito, Y., Xu, X., Han, J., Bringas, P., Jr., Maeda, T., Slavkin, H. C., Grosschedl, R. and Chai, Y. (2005). LEF1 is a critical epithelial survival factor during tooth morphogenesis. *Dev Biol* **278**, 130-143.

St-Jacques, B., Dassule, H. R., Karavanova, I., Botchkarev, V. A., Li, J., Danielian, P. S., McMahon, J. A., Lewis, P. M., Paus, R. and McMahon, A. P. (1998). Sonic hedgehog signaling is essential for hair development. *Curr Biol* **8**, 1058-1068.

Tamura, M. and Nemoto, E. (2016). Role of the Wnt signaling molecules in the tooth. *Jpn Dent Sci Rev* **52**, 75-83.

Thesleff, I., Keranen, S. and Jernvall, J. (2001). Enamel Knots as Signaling Centers Linking Tooth Morphogenesis and Odontoblast Differentiation. *Advances in Dental Research* **15**, 14-18.

Thisse, B. and Thisse, C. (2005). Functions and regulations of fibroblast growth factor signaling during embryonic development. *Developmental Biology* **287**, 390-402.

Tucker, A. and Sharpe, P. (2004). The cutting-edge of mammalian development; how the embryo makes teeth. *Nat Rev Genet* **5**, 499-508.

Tucker, A. S., Al Khamis, A. and Sharpe, P. T. (1998). Interactions between Bmp-4 and Msx-1 act to restrict gene expression to odontogenic mesenchyme. *Developmental Dynamics* **212**, 533-539.

Tummers, M. and Thesleff, I. (2009). The importance of signal pathway modulation in all aspects of tooth development. *Journal of Experimental Zoology Part B: Molecular and Developmental Evolution* **312B**, 309-319.

Vaahtokari, A., Aberg, T., Jernvall, J., Keranen, S. and Thesleff, I. (1996). The enamel knot as a signaling center in the developing mouse tooth. *Mechanisms of Development* **54**, 39-43.

Wang, X.-P., O'Connell, D. J., Lund, J. J., Saadi, I., Kuraguchi, M., Turbe-Doan, A., Cavallesco, R., Kim, H., Park, P. J., Harada, H., et al. (2009). Apc inhibition of Wnt signaling regulates supernumerary tooth formation during embryogenesis and throughout adulthood. *Development* **136**, 1939-1949.

Yokohama-Tamaki, T., Ohshima, H., Fujiwara, N., Takada, Y., Ichimori, Y., Wakisaka, S., Ohuchi, H. and Harada, H. (2006). Cessation of Fgf10 signaling, resulting in a defective dental epithelial stem cell compartment, leads to the transition from crown to root formation. *Development* **133**, 1359-1366.

Chapter 2:

Early perturbation of Wnt signaling reveals patterning and invagination-evagination control points in molar tooth development

2.1 Introduction

Developing mouse molars have long served as a model to study epithelial morphogenesis because they are simple in structure and can be easily manipulated *ex vivo* (Thesleff and Sharpe, 1997*)*. The first morphological sign of mouse molar development is a localized thickening of the dental epithelium into a placode at embryonic day (E)11.5 (Fig. 2.1A). The molar epithelium at this stage consists of distinct cell populations, including *Shh*-expressing signaling cells and more posteriorly located *Fgf8*-expressing molar epithelial progenitors (Prochazka et al., 2015). At E12.5, the placode begins to invaginate into the underlying mesenchyme. Subsequently, the dental epithelium continues to invaginate and fold into a tooth bud and then a cap-shaped structure. Concurrently, dental mesenchyme begins to condense around the bud (reviewed in Yu and Klein, 2020 and Tucker and Sharpe, 1999). Multiple rounds of reciprocal signaling between the epithelium and mesenchyme orchestrates this development.

The role of Wnt/β-catenin signaling in molar development has been the subject of a number of investigations. Hyperactivation of Wnt signaling in the molar epithelium using stabilized β-catenin or deletion of the Wnt inhibitor *Apc*, both driven by Cre recombinase under the keratin 14 (*Krt14*) promoter, led to formation of supernumerary teeth and abnormal deposits of enamel, respectively (Jarvinen et al., 2006; Wang et al., 2009; Liu et al., 2008). Conversely, hypoactivation of the Wnt pathway disrupted tooth development at various stages (Andl et al., 2002; Liu et al., 2008; Sasaki et al., 2005). Both hyperactivation and hypoactivation of Wnt/β-catenin signaling in the mesenchyme

resulted in a decrease in tooth number (Chen et al., 2009; Jarvinen et al., 2018). In humans, loss-of-function mutations of the Wnt inhibitors *APC* and *AXIN2* cause hyperdontia and hypo/oligodontia, respectively (Lammi et al., 2004; reviewed in Wang and Fan, 2011). However, beyond the notion that canonical Wnt signaling is involved in tooth formation and that it can elicit activation of other signaling pathways, the timing and precise role of the pathway in tooth morphogenesis remain unclear.

We investigated the role of canonical Wnt signaling by inactivating and hyperactivating it at earlier stages of tooth development than in any previous studies. We previously reported *Fgf8* to be strongly expressed in molar field at the initiation stage of molar development (E11.5) (Prochazka et al., 2015). Using the *Fgf8* promoter to genetically manipulate β-catenin *(Ctnnb1)*, we dialed the levels of canonical Wnt signaling up or down at E11.5, earlier than the previously used *Krt14* promoter and enriched specifically in the molar placode. This provided a more temporo-spatially specific approach to studying the role of Wnt signaling (Prochazka et al., 2015; Neubüser et al., 1997; Dassule and McMahon, 1998). Our findings indicate that the Wnt/β-catenin pathway plays an early, critical role in determining the early patterning of the tooth primordium and is likely to be a “first mover” in tooth initiation, while also showing that the level of signaling controls the relative timing of epithelial versus mesenchymal convergence movements that determine the difference between invagination and evagination, revealing this timing as a potential switch between the two forms.

2.2 Results

Wnt/β-catenin signaling is critical for initiating dental epithelial invagination and subsequent tooth formation

Wnt/β-catenin signaling is active in the *Fgf8*-enriched molar epithelium at the initiation stage (E11.5; Fig. 2.5A). To study the role of the pathway in early tooth development, we first abrogated Wnt signaling in the molar epithelium by deleting both copies of *Ctnnb1* (*Fgf8*^{CreER};*Ctnnb1*$^{fl/fl}$; hereafter called WntLOF) (Brault et al., 2001; Hoch et al., 2015). In parallel, to hyperactivate the Wnt pathway in the same population, we used a conditional *Ctnnb1* allele that is resistant to ubiquitin-mediated degradation (*Fgf8*^{CreER};*Ctnnb1*$^{\Delta ex3fl/+}$; hereafter called WntGOF) (Harada et al., 1999). In both mutants, tamoxifen was administered intraperitoneally at E10.75 to allow Cre-mediated recombination during the molar initiation stage (E11.5), as previously described (Prochazka et al., 2015).

Histology revealed that epithelial invagination was affected at E12.5 in both WntLOF and WntGOF mutants (Fig. 2.1B-G). At E11.5, the control and both mutants formed a molar placode, characterized by epithelial thickening (Fig. 2.1B-D). At E12.5, control molar placodes invaginated into the mesenchyme to form a tooth bud (Fig. 2.1E). In WntLOF, however, the molar primordium remained shallow without invaginating noticeably beyond the placodal depth (Fig. 2.1F). Strikingly, rather than invaginating into the underlying mesenchyme, the WntGOF molar epithelium evaginated into the oral cavity (Fig. 2.1G).

We used scanning electron microscopy to evaluate the WntGOF evagination in 3D. Consistent with the histological sections, WntGOF mutants at E12.5 and E14.5 displayed multiple evaginating structures scattered along the dental and vestibular surfaces instead of the shallow concavity at the molar field as seen in control and WntLOF (Fig. 2.1J-M). Histology and micro-computed tomography (μCT) of WntLOF and WntGOF mandibles at E18.5 revealed persistence of loss-of-invagination and evagination phenotypes, respectively, with neither mutant yielding any obvious tooth structure (Fig. 2.5B-D and F-H). Interestingly, the deepest invagination of the molar epithelium in *Fgf8*-driven WntGOF, which is expressed primarily in the molar progenitors, remained only slightly below the level of oral epithelium (Fig. 2.5D). The evaginating structures are prominent at multiple sites along the dental lamina, including the diastema region (Fig 2.8I and J). These phenotypes contrast with those found in previous studies, in which *Krt14* promoter-driven expression of a stabilized β-catenin throughout the oral epithelium produced hyper-invagination of the molar epithelium (Järvinen et al., 2006; Liu et al., 2008).

WntGOF caused perinatal lethality, making it impossible to follow development of the evaginating structures into the postnatal period. To circumvent this, the evaginating structures within the diastema (the toothless area between molar and incisor) of E12.5 WntGOF and littermate control mandibles were transplanted to the kidney capsule of immunocompromised mice. After 4 weeks, the explants were scanned using μCT. The control explants yielded 3 molars (2 out of 3 molars shown in Fig. 2.5I), while WntGOF explants gave rise to supernumerary teeth (*n*=2; Fig. 2.6J). This is consistent with

previous studies showing that Wnt hyperactivation induces supernumerary tooth formation (Järvinen et al., 2006; Liu et al., 2008).

β-catenin antibody staining was performed to ensure that β-catenin is abrogated and overexpressed in WntLOF and WntGOF, respectively. While there was a clear accumulation of β-catenin in evaginating molar epithelium in WntGOF, there was still lingering expression of β-catenin in the presumptive molar epithelium of WntLOF (Fig 2.8A-F). β-catenin has a dual role in signaling and cell adhesion (reviewed in Valenta et al., 2012). To determine whether inhibition of Wnt/β-catenin signaling alone is sufficient to produce the WntLOF phenotype, we chemically and genetically perturbed *Porcupine*, a member of the Wnt pathway essential for Wnt ligand secretion and activity, but not involved in cell-cell adhesion. Wildtype E11.5 mandibular explants were treated with IWP2 to pharmacologically inhibit *Porcupine*. After 24 hours, the molar placodal depth of explants treated with DMSO (vehicle control) increased 2.63 fold (*n*=15; s.d.=0.50) fold, while the placodal depth in IWP2 treated explant increased just 1.30 fold (*n*=15; s.d.=0.34) fold (Fig. 2.1N-T). Genetic abrogation of *Porcupine* in oral and dental epithelium at E11.5 using *Krt14-CreER*^{T2};*Porcn*$^{fl/f}$ also led to a delay in tooth development by E18.5 (Fig. 2.1U-X). Histological staining of *Porcn* mandible at E18.5 revealed an enamel organ, suggesting that *in vivo* the mutant can still form a tooth germ, at least up to early bell stage (Fig. 2.5E). This is consistent with a previous study that reported missing and hypoplastic teeth in *Krt14-Cre*; *Porcn*$^{fl/fl}$ mouse mutants (Liu et al., 2012). Overall the *Krt14-CreER*^{T2};*Porcn*$^{fl/fl}$ phenotype is consistent with the literature on Wnt hypomorphs in

tooth showing partial disruption of tooth formation, and its similarity to our WntLOF phenotype at early stages confirms that the latter is likely due to a loss of canonical signaling and not primarily loss of β-catenin-dependent cell adhesion.

In Wnt mutants, expression of odontogenic genes, cell proliferation and survival are perturbed.

Tooth development depends on multiple signaling pathways that mediate the dynamic interaction between the epithelium and mesenchyme. We therefore assessed the expression levels of representative members of the canonical pathways involved in odontogenesis. Whole-mount *in situ* hybridization of E11.75 mandibles (Fig. 2.6A-U) revealed that genes expressed in dental epithelium that are critical for proper tooth development (*Fgf8*, *Shh*, *Fgf4* and *Bmp4*) were downregulated in WntLOF and upregulated in WntGOF, suggesting that SHH, FGF and BMP pathways are downstream of the Wnt pathway in the early dentition, consistent with previous studies reporting that the Wnt signaling also induces both pathways in later stages of tooth development (Ahn et al., 2010). Because the controls for WntLOF and WntGOF were highly similar, representative controls are shown for each probe. SHH pathway is necessary for epithelial cell convergence and FGF for stratification, together promoting the molar epithelial invagination (Li et al., 2016). Upregulation and downregulation of *Wnt10b* expression in WntGOF and WntLOF, respectively, suggested an autoregulatory feedback loop. At E12.5, dental epithelial markers that were expressed at E11.75 were reduced in both control and WntLOF molar epithelium but persisted in the evaginating structures in

WntGOF (Fig. 2.6V-DD and KK-PP). *Msx1* and *Barx1*, which are expressed in dental mesenchyme, were downregulated in WntLOF and co-localized with the evaginating mesenchyme of WntGOF mutants, suggesting that the evaginating structures will give rise to tooth structures (Fig. 2.6J-O and EE-JJ). Furthermore, there was an overlapping expression of *Fgf8* and *Shh* within the evaginating dental epithelium (Fig. 2.6G and H).

Wnt/β-catenin signaling regulates proliferation in a number of contexts (reviewed in Clevers, 2006), and the WntGOF evagination phenotype appeared to involve extra growth. To determine if the mutants had changes in proliferation or apoptosis, EdU and TUNEL staining were performed (Fig. 2.2A-Q). In E11.5 WntLOF molar epithelium, the proportion of EdU-labeled cells significantly decreased while the number of TUNEL-labeled apoptotic cells significantly increased (Fig. 2.2 B, E, H, K, N-Q). Interestingly, EdU-labeled cells were also increased in the WntLOF molar mesenchyme. No significant difference was detected in EdU or TUNEL labeling in WntGOF mutants, in both epithelium and mesenchyme (Fig. 2.2C, F, I, L, N-Q). This indicates that Wnt/β-catenin signaling is essential for proliferation and survival of molar epithelial cells to form tooth germ, but is insufficient to perturb either mechanism when hyperactivated, suggesting that other cellular mechanisms contribute to evagination in WntGOF. In addition, there was an increase in mesenchymal cell density in both WntLOF and WntGOF mesenchyme compared to that in control at E12.5 (Fig. 2.2M).

Wnt/β-catenin signaling is required for the convergence of suprabasal cells during molar epithelial invagination

To investigate whether additional cell behaviors are altered when Wnt signaling is perturbed, we performed time-lapse microscopy on explant culture tissue slices. The *R26*$^{mT/mG}$ reporter was crossed into *Fgf8*^{CreER} (control) and *Fgf8*^{CreER};*Ctnnb1*$^{fl/fl}$ (WntLOF) to visualize molar epithelial cells. The molar placodes formed at the start of imaging (E11.5), had similar morphology in WntLOF and control (Fig. 2R and U; Movies 1 and 2). In controls, movement of epithelial cells towards the center of the placode was observed within 9 hours as the width decreased and the depth increased (Fig. 2.2R-T), consistent with previous work (Panousopoulou and Green, 2016). This cell convergence was not observed in WntLOF, resulting in a shallower placode (Fig. 2.2U-W); we were not able to image the evagination process because the presumptive evaginating sites were impossible to predict.

F-actin enrichment is associated with active cell shape changes and migration (Stricker et al., 2010), so mutant mandibles at E11.5 and E12.5 were stained for F-actin to assess if the placodal cell convergence could be driven by the active cytoskeleton of the epithelial cells themselves, as opposed to passive movement caused by external forces. At E11.5, prior to invagination, there was no F-actin enrichment in the molar placodes of the control and both mutants (Fig. 2.7A-F). By E12.5, the suprabasal layer (*i.e*. the superficial cells overlying the basal cells within the dental epithelium) of controls was highly enriched with F-actin (filled arrowheads in Fig. 2.2X and AA), consistent with previous work showing

that intercalating canopy of suprabasal cells forces the underlying cells downward (Panousopoulou and Green, 2016). In contrast, WntLOF molar epithelium did not exhibit F-actin enrichment, suggesting the loss of canopy formation (open arrowhead in Fig. 2.2Y and BB). WntGOF epithelium exhibited an increase in F-actin expression, but this appeared similar to diffuse cortical actin (arrows in Fig. 2.2Z and CC; also seen in mesenchymal cells), rather than the cable-like expression observed in the suprabasal layer of invaginating molar epithelium (Fig. 2.2X).

Evaginating mesenchyme in WntGOF mutants exhibits compromised epithelial integrity and premature mesenchymal condensation

If the WntLOF and WntGOF phenotypes are attributed to the impaired Wnt signaling, there must exist another mechanism to substitute the β-catenin in forming adherens junction, especially in WntLOF mutant. Other groups have shown that in skin, γ-catenin can compensate for the β-catenin mediated cell adhesion (Huelsken et al., 2000; Huelsken et al., 2001). Indeed, γ-catenin was expressed throughout the WntLOF dental epithelium, while γ-catenin was enriched in suprabasal layer in control, suggesting that γ-catenin may substitute for the adhesion function upon loss of β-catenin (Fig. 2.3A-B, D-E). Interestingly, there was reduced expression of γ-catenin within the evaginating epithelium in WntGOF (Fig. 2.3C and F).

E-cadherin is another essential component of adherens junctions (van Roy and Berx, 2008) that can be downregulated upon activation of Wnt/β-catenin signaling (ten Berge

et al., 2008; Jamora et al., 2003). The expression pattern of E-cadherin in the dental epithelium of control and WntLOF was comparable to that of γ-catenin (*i.e*. enriched in the suprabasal layer and uniformly expressed throughout the dental epithelium, respectively) (Fig. 2.3G-G", H-H"). Also consistent with γ-catenin expression, the E-cadherin expression in evaginating epithelium of WntGOF was reduced and localized to the suprabasal layer (Fig. 2.3I-I"), suggesting that there is a subtle reduction of cell adhesion and/or epithelial integrity in the evaginating epithelium.

Reduced molar epithelial cell-cell adhesion or mechanical stiffness in WntGOF may contribute to loss of invagination, but it does not explain how evagination occurs. Apical location of the Golgi, as marked by GM130, relative to the nucleus of the basal cells indicates that the apicobasal polarity is maintained in WntGOF (Fig. 2.7G and H; Debnath et al., 2002). We next considered whether the evagination in the WntGOF mutant might be driven not by the epithelium itself but instead by underlying mesenchyme pushing the epithelium outward into the oral cavity (Fig. 2.1G). Indeed, there was an increase in mesenchymal cell density in the evaginating mesenchyme compared to that in control at E12.5 (Fig. 2M).

We also asked whether extracellular matrix (ECM) plays a role in evagination, studying collagen VI as a representative marker. Collagen VI expression can be induced by dental mesenchymal condensation and may play a role in stabilizing the condensed mesenchyme (Mammoto et al., 2015). In control dental mesenchyme, collagen VI

expression was restricted to the basement membrane at E12.5, when the dental mesenchymal condensation initiates (Fig. 2.4A-B). By E14.5, collagen VI expression was strongly enriched within the condensed dental mesenchyme (Fig. 2.4E-F). In WntGOF, collagen VI expression was already observed in the evaginating mesenchyme at E12.5 and persisted until E14.5 (Fig. 2.4C-D, G-H). Thus, the evagination process in WntGOF mutant may be coupled to premature condensation, as well as ectopic expression of collagen VI. In addition, non-muscle myosin II has been shown to be involved in condensation of the collagenous ECM in the mouse intestine (Hughes et al., 2019). In the control molar mesenchyme, there was circumferential expression of phospho-myosin light chain (pMLC) that parallels the curvature of the basement membrane (Fig. 2.3J and M), whereas this expression was absent in the WntLOF mesenchyme (Fig. 2.3K and N). Interestingly, the pMLC expression in the WntGOF embryos showed myosin activity in the evaginating mesenchyme (Fig. 2.3L and O). Furthermore, *Msx1*, which is strongly expressed control dental mesenchyme at E14.5, was upregulated in WntGOF mesenchyme where evaginating structures are located, suggesting that the evaginating mesenchymal cells have odontogenic potential (Fig. 2.9A and B). Interestingly, hyperactivating Wnt/β-catenin pathway in dental mesenchyme via *Msx1*-promoter driven *Ctnnb1*$^{\Delta ex3fl/+}$ perturbed the tooth germ formation by E14.5, but it did not affect the invagination of molar epithelium into the underlying mesenchyme (Fig. 2.9C and D).

To test whether increased collagenous ECM contributes to evagination, we pharmacologically inhibited collagen synthesis in E11.5 WntGOF and control mandibles.

Each mandible was bisected, and one hemimandible treated with the collagen synthesis inhibitor Mithramycin A (Mit A) (Blume et al., 1991; Ihn et al., 2001) and the other with vehicle (DMSO) (Fig. 2.4I). After 48 hours of culture, Mit A treatment partially prevented both invagination of control molar placode and evagination in WntGOF. However, the decrease in height of evagination in WntGOF was significantly greater than the depth reduction of molar epithelial invagination in control (Fig. 2.4J-N). As expected, there was a decrease in overall collagen VI expression in the explants treated with Mit A, compared to the vehicle control (Fig. 2.7I-L). This suggested that the premature and dysregulated accumulation of ECM proteins, such as collagen VI, promotes evagination in WntGOF mutants through increasing local mesenchymal stiffness along with premature increased cell density. One potential caveat to these results is that although it is frequently used to inhibit collagen synthesis, Mit A may affect other biological processes as well.

2.3 DISCUSSION

An accumulation of tooth mutant phenotypes has, over the years, established that Wnt/β-catenin signaling is an integral part of the regulatory signaling network of tooth development. However, exactly how Wnt/β-catenin signaling regulates tooth development – not just the signaling but also the morphogenesis – has remained unclear. Previous studies have been carried out by either global or pan-epithelial manipulation of the Wnt/β-catenin pathway, which resulted in blockage of tooth development at various late stages. The discrepancy in phenotypes resulting from the perturbation of the same pathway has obscured the precise role of Wnt signaling in tooth development. The reason

for the different phenotypes in previous studies is likely due to the difference in the temporo-spatial specificity of the Cre drivers. Here, we found that abrogating Wnt/β-catenin signaling in *Fgf8*-enriched molar epithelium almost completely prevented the molar placode from invaginating into the underlying mesenchyme, thereby resulting in near deletion of the tooth germ. This indicates that Wnt/β-catenin signaling is essential for epithelial invagination at the earliest stages. We observed several cellular processes that may contribute to the WntLOF phenotype, including a decrease in cell proliferation and survival. Live imaging data revealed that the overall movement of molar epithelial cells towards the midline of the placode was lost upon abrogation of the Wnt pathway, which may drive the WntLOF phenotype. Our data also indicate that the Wnt pathway lies upstream of SHH, FGF and BMP signaling. It has been published that the SHH and FGF pathways promote cell convergence in the suprabasal cell layer and cell proliferation of embryonic molar, respectively (Li et al., 2016). In WntLOF, both SHH and FGF pathways are downregulated, and this may mediate the loss of invagination of molar epithelium.

We have also refined our understanding of the Wnt pathway's role during early tooth development through hyperactivating the pathway in specific tissue and time. The evaginating tooth germ in the WntGOF mutants resembles those found in early tooth development of paddlefish, alligators and turtles (Kozawa et al., 2005; Smith et al., 2015; Tokita et al., 2013). It also resembles the evaginations observable, but rarely noted, that raise feather buds and some hair follicles such as the vibrissae (whiskers) above surrounding skin. Our findings suggest that premature mesenchymal condensation in

WntGOF may push the epithelium outward as it compacts around the presumptive tooth sites.

The mechanisms underlying mesenchymal condensation are not fully understood, including the temporal relationships between cell density, tissue stiffness, and cell movement. In addition to cell compaction, it is possible that other features of mesenchymal condensation, such as production of ECM, also play a role. Expression of collagen VI, a known marker for dental mesenchymal condensation, was restricted to the basement membrane at E12.5 in control. Premature collagen VI expression in WntGOF suggests dysregulated mesenchymal condensation. Indeed, there was a significant increase in cell density within the evaginating mesenchyme of WntGOF at E12.5, compared to that of control tooth germ at E12.5. Interestingly, collagen VI has also been reported to be associated with Bethlem myopathy and Ullrich congenital muscular dystrophy in humans (Baker et al., 2007; Baker et al., 2005). These patients have irregular, crowded dentition, further suggesting its role as an ECM protein in dental mesenchyme during tooth development. Furthermore, mesenchymal condensation has also been observed in other organs that develop through evagination, such as feather buds and intestinal villi (Widelitz et al., 2003; Hughes et al., 2018; Shyer et al., 2017). The compaction of dental mesenchyme is crucial in shaping the cervical loops of molar tooth germ (Marin-Riera et al., 2018; Morita et al., 2016). A simple change in the timing of cell convergence in the epithelium and cell convergence (condensation) in the mesenchyme

could act as an evolutionary switch between evagination and invagination, regulated as simply as by changing the strength of canonical Wnt signaling.

Lastly, it is notable that the location of evagination sites in WntGOF appeared to be stochastic, as opposed to predictable and sequential sites of molar tooth germ in control. One simple explanation could be that the elevated Wnt signaling promotes the survival and proliferation of *Fgf8*+ cells, a well-known role of Wnt signaling in various tissue contexts. However, although the ectopic evagination locations appeared random, they were always well-spaced. These phenotypes are consistent with a residual periodic reaction-diffusion (RD)-type mechanism. Spatial and temporal patterning of tooth germs has long been theorized to be patterned *via* an RD system (Murray and Kulesa, 1996; Sadier et al., 2019). Indeed, members of the Wnt pathway have been shown to pattern spacing *via* RD in the hair follicle (Sick et al., 2006) and, more recently, experiments and modelling have reinforced this idea for molar patterning (Sadier et al., 2019). If this is the case, then our results indicate that Wnt is a likely participant in the core RD network that initiates the tooth germ, and the proper balance of signaling through this network ultimately dictates whether an invagination or an evagination will form. Through control of this essential early step in tooth formation, titration of levels of Wnt signaling ensures that subsequent stages of morphogenesis have the correct building blocks to work with.

2.4 MATERIALS AND METHODS

Mouse genetics

All animal experiments were performed in accordance with the guidelines established by Institutional Animal Care and Use Committee (IACUC) and Laboratory Animal Resource Center (LARC) of University of California, San Francisco, CA, USA. The following mouse strains were used: C57BL/6J (Jackson Laboratory: 000664); *Fgf8*^{CreER} (Hoch et al., 2015); *Krt14-CreER*^{T2} (MGI: 2177426); *Porcn*^{flox} (MGI: 1890212); *Ctnnb1*$^{\Delta ex3fl/+}$ (MGI: 1858008); *Ctnnb1*^{flox} (MGI: 2148567); *R26*$^{mT/mG}$ (MGI: 3716464); *BAT-GAL* (MGI: 3697064); *Foxn1*^{nu} (immunocompromised mice; Jackson Laboratory: 007850). For generation of embryos and kidney capsule transplant, 6- to 8-week-old animals were used for breeding. Tamoxifen (0.2 mg/g of body weight) was administered via intraperitoneal (IP) injection to pregnant dams at E10.75 to induce genetic recombination by the initiation stage (E11.5). Each experiment was performed at least three times with different embryos. The following developmental features were used as references to confirm the stages of the harvested embryos: E11.5 – visible auditory hillocks, round anterior foot plates, fusion of two lateral lingual swellings; E12.5 – interdigital indentations without clear separation of digits, separation of the tongue from the oral epithelium.

EdU and TUNEL staining and quantification

The mice at E11.5 of pregnancy were administered with EdU (Invitrogen, C10637; 1mg/25 g body weight) via IP injection 1 h before euthanasia. All the harvested embryos

were fixed in 4% paraformaldehyde (PFA) at 4°C at the same time immediately after decapitation. Following overnight fixation, mandibles were isolated and sectioned for subsequent analysis. EdU detection was performed according to standard protocol provided by the EdU detection kit (Thermo Fisher Scientific, C10338). The total number of nuclei and the EdU+ nuclei were counted in seven sequential sections, and the proportion of EdU+ nuclei to the total number of nuclei was used for quantitative analyses. As for the mesenchyme, region of analysis was defined to include five to six layers of mesenchymal cells from the basement membrane surrounding the invaginating epithelium.

For TUNEL staining, sections were deparaffinized, rehydrated and incubated in 0.1% trypsin solution at 37°C for 14 min. The *In Situ* Cell Death Detection Kit, TMR red (Roche, 12156792910) was used according to manufacturer's instructions. Positive and negative controls were included per manufacturer's instruction. The total number of TUNEL-stained nuclei from seven sequential sections was counted for quantitative analyses. The EdU and TUNEL counts were comparable between the WntLOF control and WntGOF controls and were thus pooled for counting.

To calculate mesenchymal cell density, the mesenchymal area for counting was defined as explained above, and all of the nuclei within the defined parameter were counted. Cell density was calculated by dividing the number of nuclei by a defined area, which is automatically calculated by Fiji software.

X-gal staining and section in situ hybridization

Mandibles were harvested from BAT-GAL embryos at E11.5 and fixed in Mirsky's fixative (National Diagnostics) overnight and subsequently stained in X-Gal solution. Stained samples were rinsed, post-fixed in 4% PFA and paraffin-sectioned for subsequent *in situ* hybridization. *In situ* hybridization to detect Fgf8 expression was performed using DIG-labeled probes using a protocol modified from Riddle et al. (1993). Modifications are detailed under Whole-mount *in situ* hybridization section.

Kidney capsule graft

The portion of the mandibles containing the evaginating structures was dissected from E12.5 WntGOF embryos and transplanted under the renal capsule of immunocompromised mice (*Foxn1*^{nu}). The equivalent region of littermate controls, including the molar tooth germs, were used as controls. The analgesics were administered according to the IACUC guidelines. The mice were anesthetized by isoflurane inhalation. Aseptic techniques were practiced for surgery. A longitudinal incision of 1-1.5 cm was made to exteriorize the kidney. One tooth germ was transplanted under the kidney capsule per animal. The peritoneum and skin were closed with suture. The mice were then placed under a heat lamp for recovery and monitored until fully awake. The mice were euthanized for retrieval of the grafts for analyses 4 weeks post-surgery, and the grafts were scanned using μCT.

Micro-computed X-ray tomography

Samples were scanned using MicroXCT-200 (Carl Zeiss Microscopy). The harvested renal grafts were gradually dehydrated to 70% ethanol and scanned at 40 kV and 200 μA. We took 800 projection images at a total integration time of 12 s with linear magnification of 4 and a pixel size of 5.4 μm. For imaging of the E18.5 heads, samples were additionally soaked in phosphotungstic acid overnight to differentially stain soft tissues as described in Metscher (2009) and scanned at 60 kV and 200 μA. We took 1200 projection images at a total integration time of 4 s, with linear magnification of 4 and a pixel size of 4.4μm. Images were analyzed using Avizo (FEI).

Whole-mount in situ hybridization

Embryonic mandibles were fixed in 4% PFA overnight at 4°C. *In situ* hybridization was performed using a protocol modified from Riddle et al. (1993). Prior to *in situ* hybridization, all samples were dehydrated through graded methanol and stored at −20°C until further use. Immediately prior to *in situ* hybridization, samples were gradually rehydrated to DEPC-treated PBST (PBS with 0.1% Tween 20) and incubated in 6% hydrogen peroxide. The subsequent steps are as described by Riddle et al. (1993).

The plasmids for the generation of RNA probes were kind gifts of Drs I. Thesleff (*Wnt10b*), G. Martin (*Fgf8*, *Shh*, *Msx1*, *Fgf4* and *Bmp4*) and T. Mitsiadis (*Barx1*). To generate antisense probes, plasmids were linearized with the appropriate restriction

enzymes (RE) and transcribed using RNA polymerase (RNAP) with RNA-DIG labeling mix (Roche). RNA probes were precipitated and resuspended in RNAase-free water. DIG-labeled RNA probes were transcribed in vitro from plasmids containing: *Wnt10b*, *Fgf8*, *Shh*, *Msx1*, *Barx1*, *Fgf4* and *Bmp4*.

Live imaging

The *R26*$^{mT/mG}$ reporter was crossed into *Fgf8*^{CreER} (control) and *Fgf8*^{CreER}; *Ctnnb1*$^{fl/fl}$ (WntLOF) to visualize molar epithelial cells. Embryonic mandibles were harvested at E11.5. From each mandible, two incisions near the lateral borders of the tongue were introduced to remove tongue primordium and generate two hemi-mandibles. The hemi-mandibles were manually sliced to generate a frontal section through the molar placode for imaging. The explants were embedded and cultured in 0.3% low melting point agarose medium for the entire duration of the imaging as described in Prochazka et al., 2015. Live imaging was performed using a CSU-X1 Yokogawa spinning disk confocal unit on an inverted Zeiss Observer Z1 microscope.

Immunofluorescence and Phalloidin staining

Immunofluorescence was performed on paraffin sections and cryosections. Paraffin sections were de-paraffinized and rehydrated. Antigen retrieval was performed by sub-boiling slides in a microwave for 15 min in a citrate buffer (pH 6.2) containing 10 mM citric acid, 2 mM EDTA and 0.05% Tween-20. Samples were blocked in animal-free

blocker (Vector Laboratories, SP-5030) supplemented with 2.5% heat-inactivated goat serum, 0.02% SDS and 0.1% Triton X-100. Anti-collagen VI (Abcam, ab182744), anti-pMLC (Abcam, ab2480), anti- γ-catenin (Abcam, ab184919), anti-E-cadherin (Cell Signaling Technology, 3195S) and anti-GM130 (Cell Signaling Technology, 2296S) primary antibodies were used. All of the antibodies were diluted 1:300 in the same blocking solution without serum. For Phalloidin staining, embryos were fixed in 4% PFA overnight at 4°C, graded to 30% sucrose, embedded in OCT and cryo-sectioned. Sections were stained with Alexa Fluor™594 (Thermo Fisher Scientific, A12381) according to the manufacturer's protocol. DAPI (Invitrogen, D1306) was used to stain nuclei for immunofluorescence and Phalloidin staining. All of the images were acquired using CSU-X1 Yokogawa spinning disk confocal unit on an inverted Zeiss Observer Z1 microscope.

Histology

Embryonic mandibles were fixed in Bouin's fixative overnight at room temperature, paraffin-sectioned, dehydrated through graded ethanol concentrations, deparaffinized with Histoclear (National Diagnostics), rehydrated through an ethanol gradient, stained with Hematoxylin and Eosin, dehydrated through an ethanol gradient, incubated in histoclear, and mounted using Permount (Fisher Scientific).

SEM

Harvested embryonic mandibles were fixed in 4% PFA and gradually dehydrated to 100% ethanol. Samples were subject to critical point drying, mounted to SEM sample stub and sputtered with gold-palladium. Scanning electron micrographs were obtained using a JEOL JCM-5000 Neoscope Scanning Electron Microscope. All SEM was performed at the University of California, San Francisco DRC Microscopy core.

Pharmacological inhibition assay

Embryonic mandibles were harvested at E11.5 and bisected. The left hemimandible was treated with DMSO and the right side with 250 nM Mit A (Tocris, #1489). Each hemimandible was embedded in Matrigel (356231, Corning) on a cell culture insert (Millicell) in a 12-well plate. Explants were cultured at the interface of air and media, comprising DMEM/F12 (Gibco), 20% fetal bovine serum, 1% glutamine, and 1% penicillin/streptomycin, at 37°C and 5%CO2. After 48 h of culture, explants were rinsed, fixed with 4% PFA and embedded in 6% low-melting agarose (Invitrogen). Fixed samples were then vibratome-sectioned at thickness of 50 μm and imaged using a Leica DMi8 S platform live cell microscope. The depth of dental epithelial invagination or evagination was measured from the center of the suprabasal layer vertically to the expanded dental epithelium.

Statistical analysis

Data are expressed as mean±s.d. Two-tailed paired Student's t-tests were used for EdU and TUNEL staining, mesenchymal cell density, IWP2 data and Mit A inhibition data.

2.5 Acknowledgments

We thank A. Rathnayake, B. Hoehn and S. Alto for technical assistance, and Drs. Pauline Marangoni, Teemu Hakkinen, and other members of the Klein and Green labs for helpful discussions. This work was supported by NIH R01-DE028496 to O.D.K and J.B.A.G. and NIH R35-DE026602 to O.D.K.. R.K. was supported by NIH F30-DE025160.

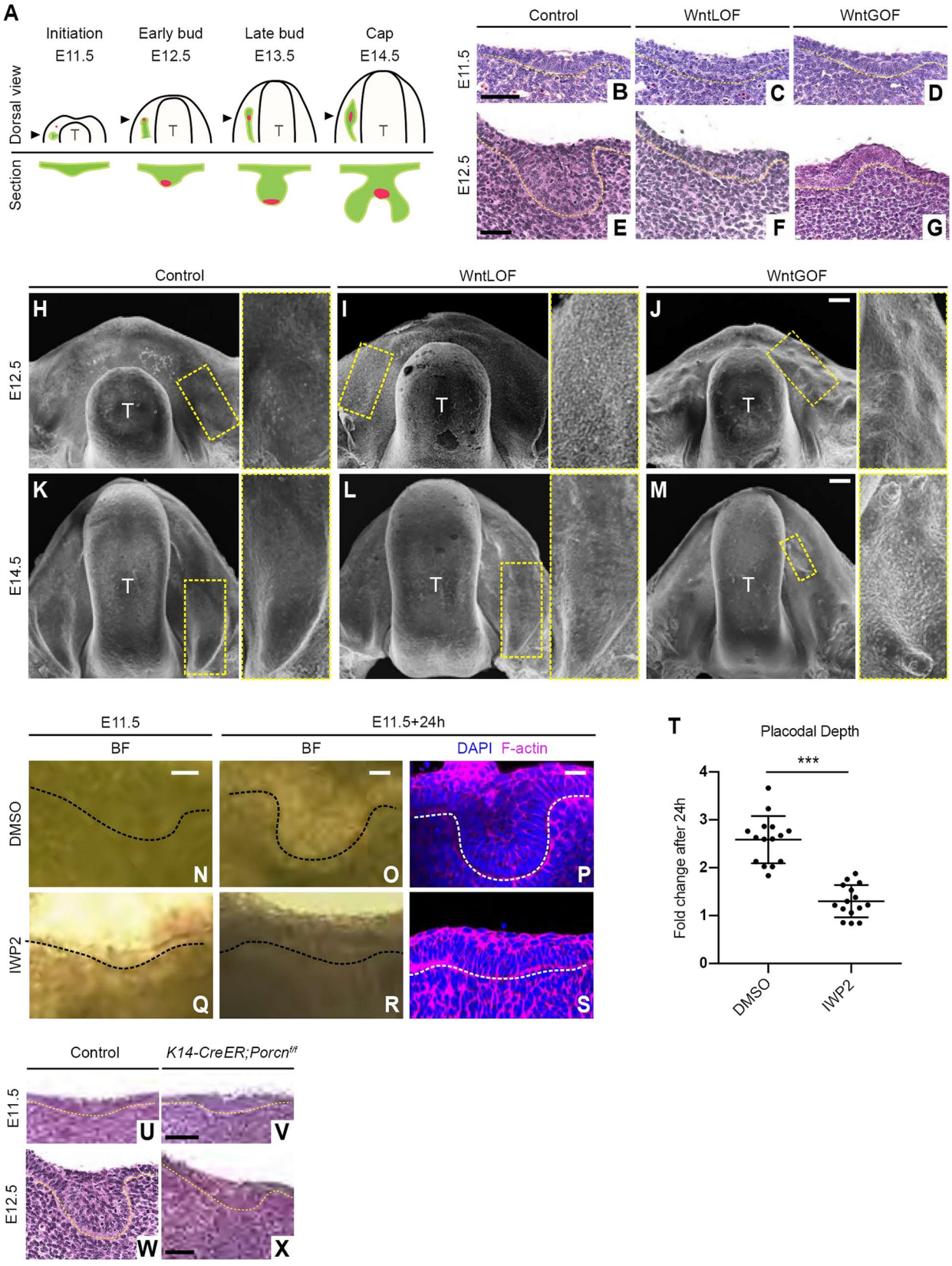
A
Initiation
E11.5
Early bud
E12.5
Late bud
E13.5
Cap
E14.5
Dorsal view
Section
T
Control
WntLOF
WntGOF
E11.5
E12.5
B
C
D
E
F
G
H
I
J
K
L
M
E14.5
E11.5+24h
BF
DAPI F-actin
DMSO
IWP2
N
O
P
Q
R
S
T
Placodal Depth
***
Fold change after 24h
DMSO
IWP2
K14-CreER;Porcn f/f
U
V
W
X

Figure 2.1. Proper Wnt signaling in *Fgf8+* population is required for dental epithelial invagination. (A) Schematic of early mouse molar development. Green, *Fgf8*-enriched molar field; red, signaling center. (B-G) Frontal histological sections through molar tooth germ at E11.5 and E12.5. (H-M) Oral surface view of E12.5 and E14.5 mandibles using scanning electron microscope. T, tongue. Inset (right) shows magnification of yellow boxed area. (N-S) Frontal section of E11.5 mandible cultured for 24 h with DMSO (vehicle) or IWP2. BF, brightfield. (T) Quantification of fold change in placodal depth after IWP2 treatment. Data are mean ±s.d. n=15. ***P<0.01 (two-tailed paired Student's t-test). (U-X) Histological sections through molar tooth germ at E11.5 and E12.5 in control and *Porcn* mutant. Dashed lines indicate epithelial-mesenchymal border. Scale bars: 50 μm (B-G,N-X); 100 μm (H-J); 200 μm (K-M).

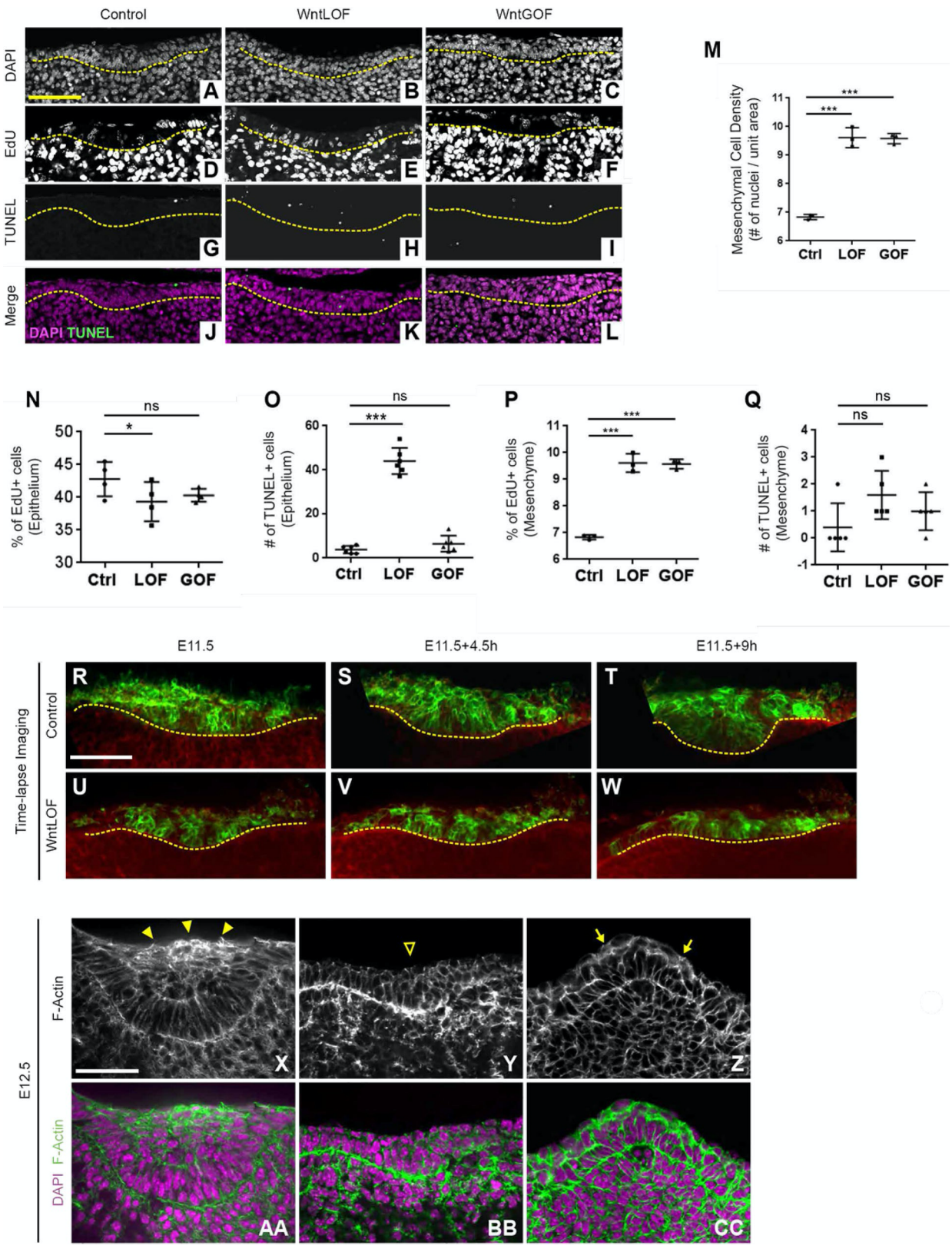
Control
WntLOF
WntGOF
DAPI
EdU
TUNEL
Merge
DAPI TUNEL
A
B
C
D
E
F
G
H
I
J
K
L
M
Mesenchymal Cell Density
(# of nuclei / unit area)
Ctrl
LOF
GOF
N
% of EdU+ cells
(Epithelium)
O
# of TUNEL+ cells
(Epithelium)
P
% of EdU+ cells
(Mesenchyme)
Q
# of TUNEL+ cells
(Mesenchyme)
ns
E11.5
E11.5+4.5h
E11.5+9h
Time-lapse Imaging
Control
WntLOF
R
S
T
U
V
W
E12.5
F-Actin
DAPI F-Actin
X
Y
Z
AA
BB
CC

Figure 2.2. Wnt signaling is required for cell proliferation and survival, and medial movement of suprabasal cells. (A-L) Representative image of DAPI, EdU and TUNEL staining in molar tooth germ at E11.5. (M) Quantification of nuclear density in E12.5 molar mesenchyme. (N-Q) Quantification of the average percentage of EdU-stained cells and total number of TUNEL-stained cells in seven sequential sections. (R-W) Time lapse imaging of E11.5 mandible slice culture of control and WntLOF. Green, dental epithelial cells; red, non-dental epithelial cells. Yellow dashed line, epithelial-mesenchymal border. (X-CC) F-actin staining of presumptive tooth germ at E12.5. Filled arrowhead, F-actin enrichment; open arrowhead, absence of F-actin enrichment; arrow, cortical-actin-like F-actin expression. Data are mean±s.d. For M-Q, **P*<0.05. ****P*<0.01 (two-tailed paired Student's *t*-test). ns, statistically not significant. Scale bars: 50 μm.

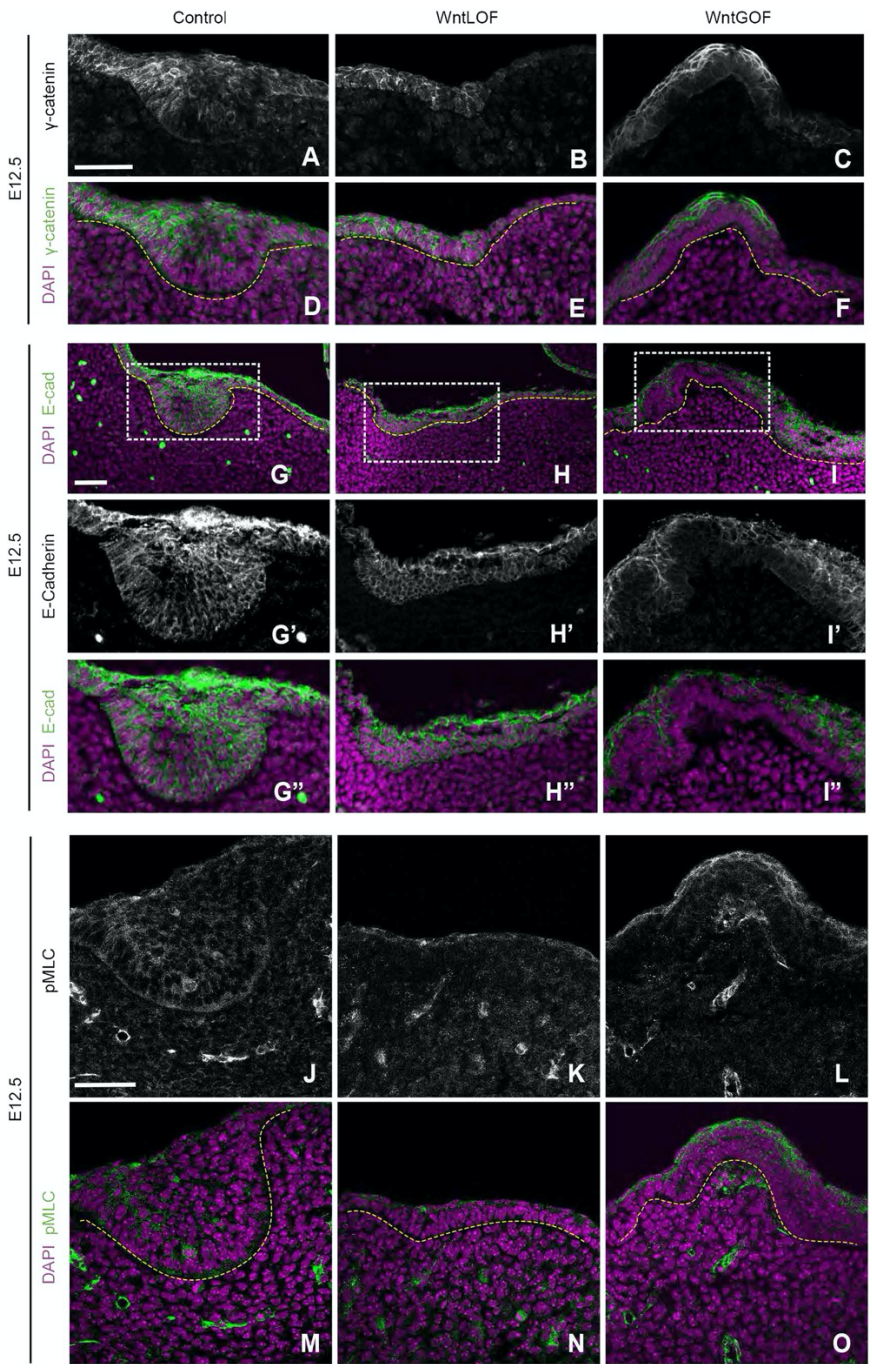

Figure 2.3. Reduced epithelial actin bundles and E-cadherin expression in evaginating structure. (A-F) γ-Catenin staining of presumptive tooth germ in control, WntLOF and WntGOF at E12.5. (G-I″) E-cadherin expression in E12.5 presumptive tooth germ. G′,G″, H′,H″ and I′,I″ show magnifications of boxed areas in G,H and I, respectively. (J-O) pMLC expression in E12.5 presumptive tooth germ. Yellow dashed line, epithelial- mesenchymal border. Scale bars: 50 μm

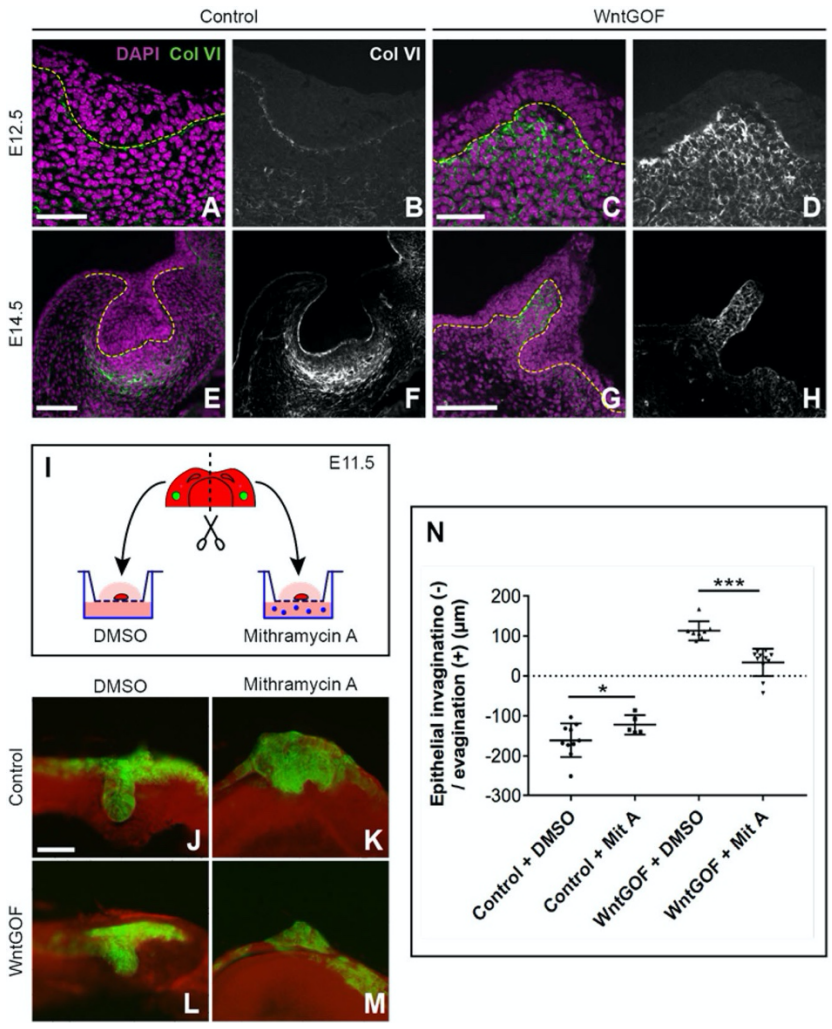

Figure 2.4. Premature collagen VI expression is observed in evaginating structures and contributes to evagination phenotype. (A-H) Immunofluorescence of collagen VI (Col VI) at E12.5 and E14.5 in control and WntGOF. Yellow dashed line, epithelial-mesenchymal border. (I) Schematic of explant culture experiment. (J-M) Frontal section of presumptive tooth germs after 48 h. Green, dental epithelial cells; red, non-dental epithelial cells. (N) Quantification of fold change in placodal depth after Mit A treatment. Data are mean±s.d. *P<0.05, ***P<0.01 (two-tailed paired Student's t-test). Scale bars: 50 µm.

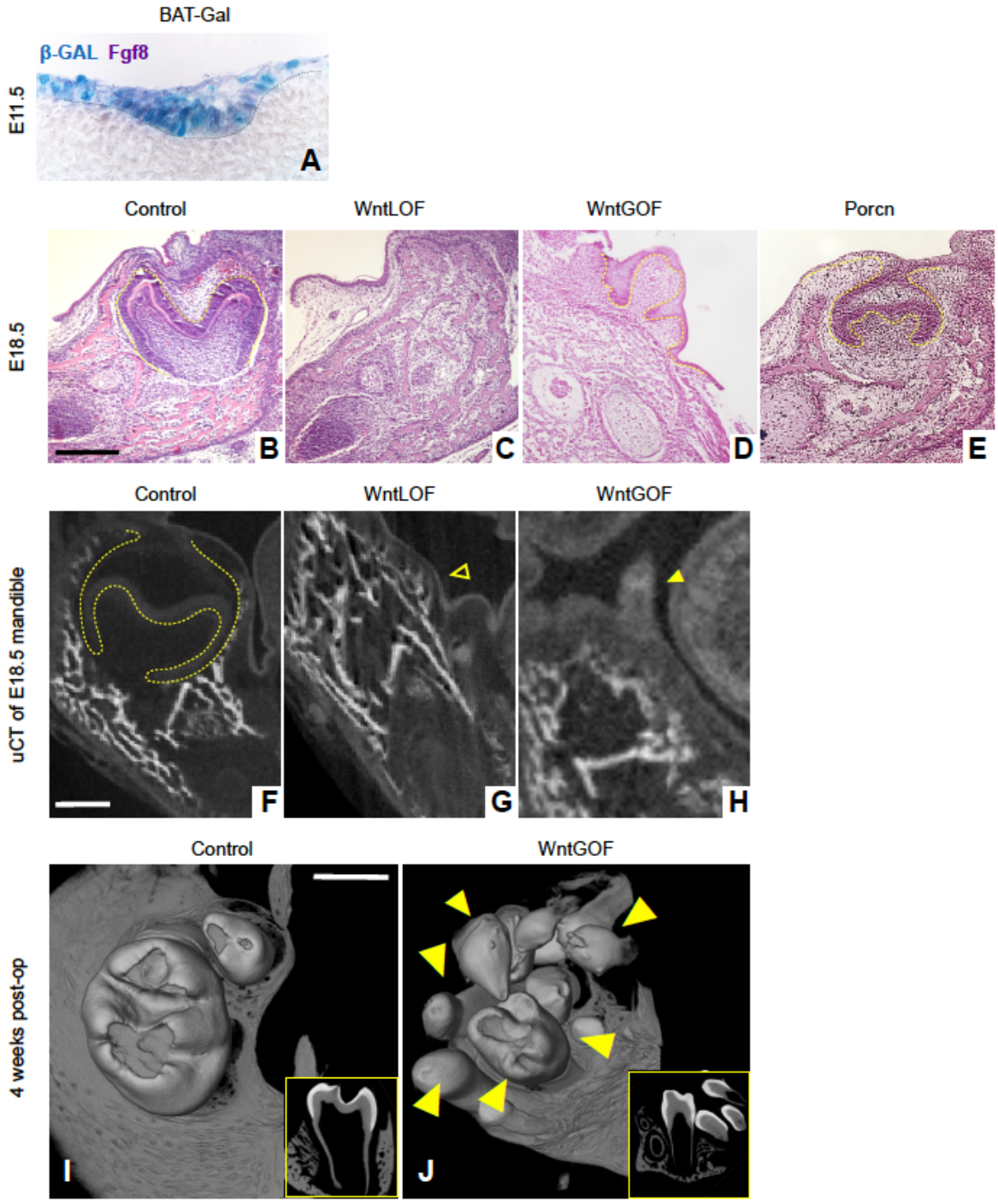
BAT-Gal
β-GAL Fgf8
E11.5
A
Control
WntLOF
WntGOF
Porcn
E18.5
B
C
D
E
Control
WntLOF
WntGOF
uCT of E18.5 mandible
F
G
H
Control
WntGOF
4 weeks post-op
I
J

Figure 2.5. WntLOF leads to anodontia and WntGOF induces supernumerary teeth formation. (A) Co-localization of *BAT-GAL* and *Fgf8* mRNA expression. (B-H) Histological sections (B-E) and μCT (F-H) of presumptive molar field at E18.5. Yellow dotted line: epithelial- mesenchymal border. Open arrowhead, presumptive molar site in WntLOF (G). Filled arrowhead,evaginating structure in WntGOF (H). (I and J) μCT of explants of WntGOF and littermate control4 weeks post-renal graft. Scale bar: 100 μm for B-H; 500 μm for I and J.

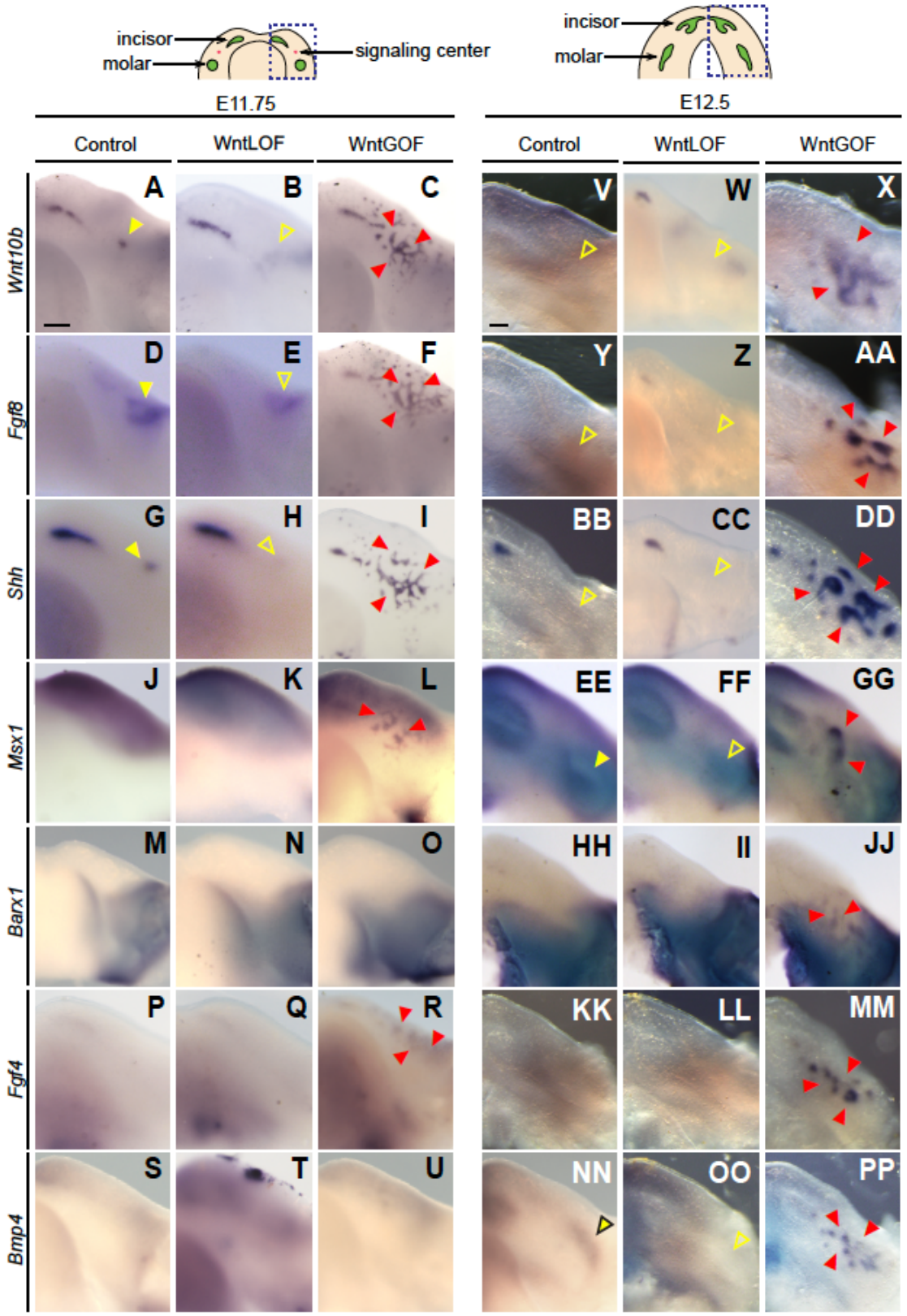
incisor
molar
signaling center
E11.75
incisor
molar
E12.5
Control
WntLOF
WntGOF
Control
WntLOF
WntGOF
Wnt10b
Fgf8
Shh
Msx1
Barx1
Fgf4
Bmp4
A
B
C
V
W
X
D
E
F
Y
Z
AA
G
H
I
BB
CC
DD
J
K
L
EE
FF
GG
M
N
O
HH
II
JJ
P
Q
R
KK
LL
MM
S
T
U
NN
OO
PP

Figure 2.6. Expression of odontogenic genes are perturbed in WntGOF and WntLOF mutants. (A-PP) Oral surface view of odontogenic gene expressions in control, WntLOF and WntGOF at E11.75 (A-U) and E12.5 (V-PP). Filled yellow arrowheads, expression in molar tooth germ (D and BB) and signaling center (A and G). Red arrowheads, ectopic expression. Open arrowheads, reduced expression. Scale bar 1mm.

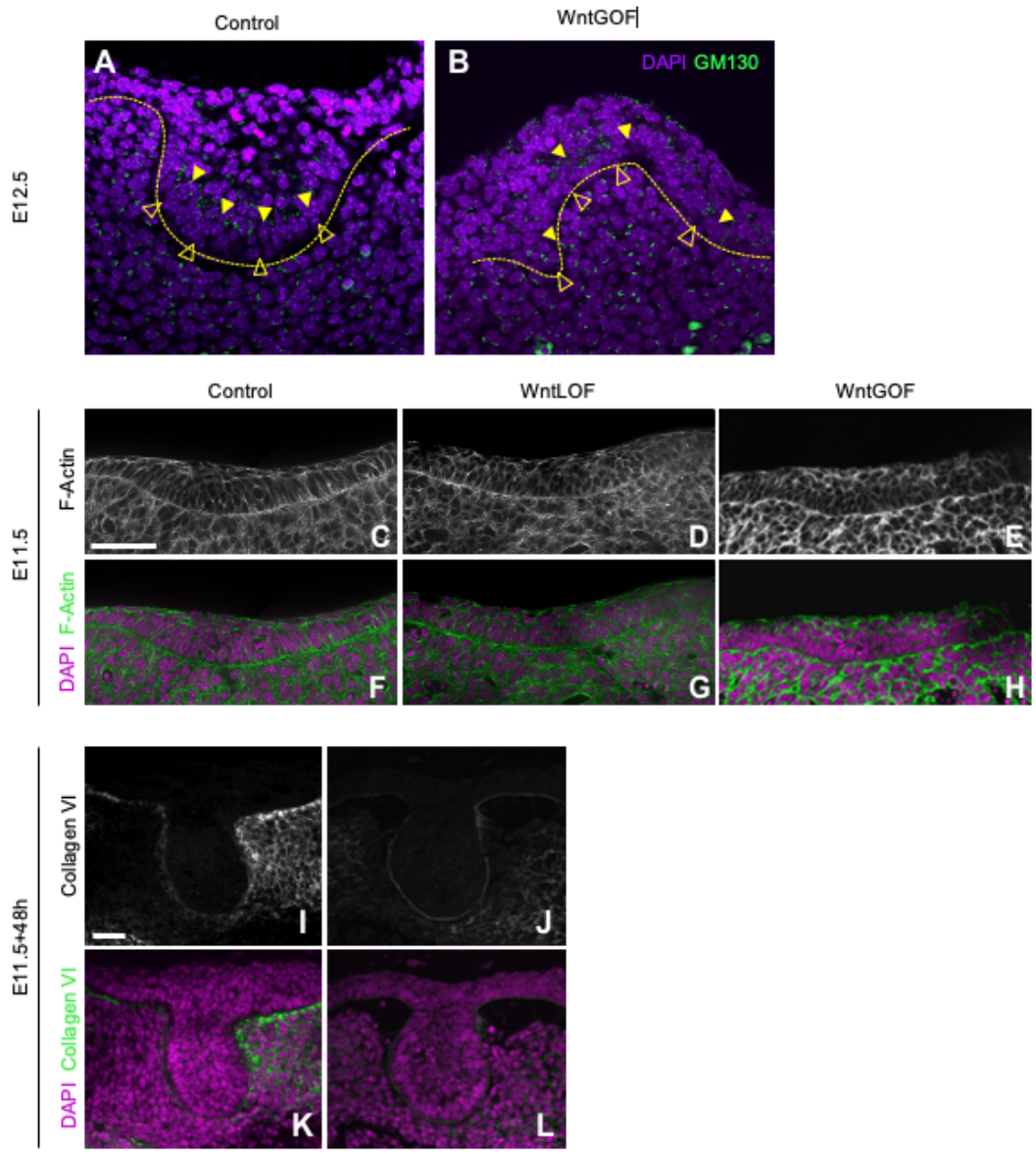

Figure 2.7. The epithelial basoapical polarity is maintained in WntGOF and Mithramycin A inhibits collagen VI expression. (A-B) GM130 expression in E12.5 tooth germ in control and WntGOF. Closed arrowhead, GM130. Open arrowhead, basal cell nuclei. (C-H) F-actin staining of presumptive tooth germ of control, WntLOF and WntGOF at E11.5. (I-L) Collagen VI expressionin Mithramycin A treated control explants at E11.5+48h. Scale bar: 50 μm for A-L.

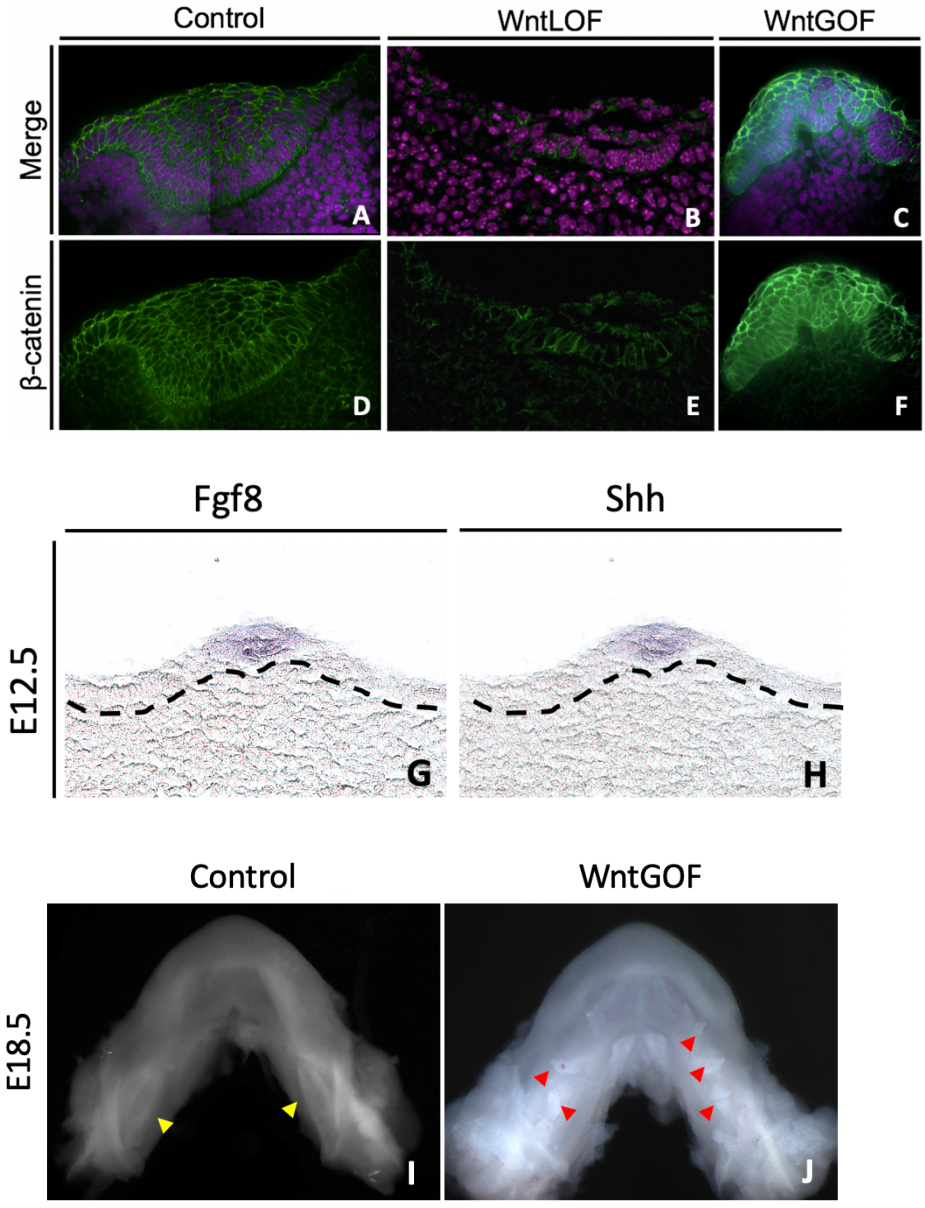

Figure 2.8. Epithelial expression of Fgf8 and Shh overlap within the evaginating structure in WntGOF. (A-F) β-catenin expression in E12.5 presumptive tooth germ in and WntGOF. (G and H) *Fgf8* and *Shh* mRNA expression in tandem sections of evaginating structure in E12.5 WntGOF. Dotted line, epithelial-mesenchymal border. (I and J) Oral surface view of E18.5 control and WntGOF mandible under dissection scope (tongue is surgically removed). Yellow arrowhead, molar tooth germ. Red arrowhead, evaginating structure.

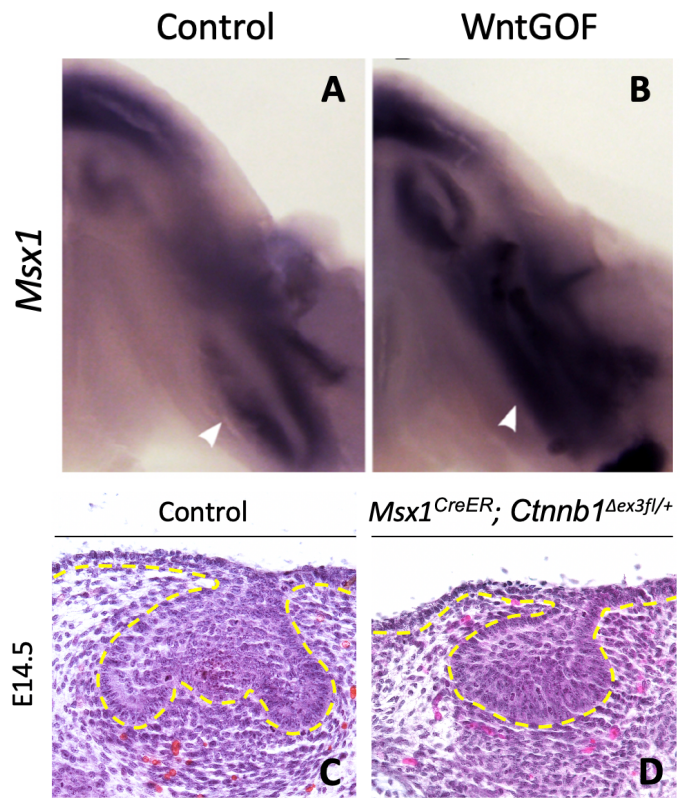

Figure 2.9. Increased Wnt/β-catenin signaling in dental mesenchyme perturbs odontogenesis. (A and B) Oral surface view of *Msx1* in control and WntGOF at E14.5. Arrowhead, presumptive dental mesenchyme. (C and D) Frontal histological sections through molar tooth germ at E14.5 in control and *Msx1*^{CreER};*Ctnnb1*$^{\Delta ex3fl/+}$. Yellow dotted line, epithelial-mesenchymal border.

2.6 References

Ahn, Y., Sanderson, B. W., Klein, O. D. and Krumlauf, R. (2010). Inhibition of Wnt signaling by Wise (Sostdc1) and negative feedback from Shh controls tooth number and patterning. *Development* **137**, 3221-3231.

Andl, T., Reddy, S. T., Gaddapara, T. and Millar, S. E. (2002). WNT signals are required for the initiation of hair follicle development. *Dev Cell* **2**, 643-653.

Baker, N. L., Morgelin, M., Pace, R. A., Peat, R. A., Adams, N. E., Gardner, R. J., Rowland, L. P., Miller, G., De Jonghe, P., Ceulemans, B., et al. (2007). Molecular consequences of dominant Bethlem myopathy collagen VI mutations. *Ann Neurol* **62**, 390-405.

Baker, N. L., Morgelin, M., Peat, R., Goemans, N., North, K. N., Bateman, J. F. and Lamande, S. R. (2005). Dominant collagen VI mutations are a common cause of Ullrich congenital muscular dystrophy. *Hum Mol Genet* **14**, 279-293.

Brault, V., Moore, R., Kutsch, S., Ishibashi, M., Rowitch, D. H., McMahon, A. P., Sommer, L., Boussadia, O. and Kemler, R. (2001). Inactivation of the beta-catenin gene by Wnt1-Cre-mediated deletion results in dramatic brain malformation and failure of craniofacial development. *Development* **128**, 1253-1264.

Calamari, Z. T., Hu, J. K. and Klein, O. D. (2018). Tissue Mechanical Forces and Evolutionary Developmental Changes Act Through Space and Time to Shape Tooth Morphology and Function. *Bioessays* **40**, e1800140.

Chen, J., Lan, Y., Baek, J. A., Gao, Y. and Jiang, R. (2009). Wnt/beta-catenin signaling plays an essential role in activation of odontogenic mesenchyme during early tooth development. *Dev Biol* **334**, 174-185.

Clevers, H. (2006). Wnt/beta-catenin signaling in development and disease. *Cell* **127**, 469-480.

Dassule, H. R. and McMahon, A. P. (1998). Analysis of epithelial-mesenchymal interactions in the initial morphogenesis of the mammalian tooth. *Dev Biol* **202**, 215-227.

Debnath, J., Mills, K. R., Collins, N. L., Reginato, M. J., Muthuswamy, S. K., & Brugge, J. S. (2002). The role of apoptosis in creating and maintaining luminal space within normal and oncogene-expressing mammary acini. *Cell, 111*(1), 29-40.

Harada, N., Tamai, Y., Ishikawa, T., Sauer, B., Takaku, K., Oshima, M. and Taketo, M. M. (1999). Intestinal polyposis in mice with a dominant stable mutation of the beta-catenin gene. *EMBO J* **18**, 5931-5942.

Hoch, R. V., Clarke, J. A. and Rubenstein, J. L. (2015). Fgf signaling controls the telencephalic distribution of Fgf-expressing progenitors generated in the rostral patterning center. *Neural Dev* **10**, 8.

Huelsken, J., Vogel, R., Brinkmann, V., Erdmann, B., Birchmeier, C. and Birchmeier, W. (2000). Requirement for beta-catenin in anterior-posterior axis formation in mice. *J Cell Biol* **148**, 567-578.

Huelsken, J., Vogel, R., Erdmann, B., Cotsarelis, G. and Birchmeier, W. (2001). β-Catenin Controls Hair Follicle Morphogenesis and Stem Cell Differentiation in the Skin. *Cell* **105**, 533-545.

Hughes, A. J., Miyazaki, H., Coyle, M. C., Zhang, J., Laurie, M. T., Chu, D., Vavrusova, Z., Schneider, R. A., Klein, O. D. and Gartner, Z. J. (2018). Engineered Tissue Folding by Mechanical Compaction of the Mesenchyme. *Dev Cell* **44**, 165-178 e166.

Ihn, H., Ihn, Y. and Trojanowska, M. (2001). Spl phosphorylation induced by serum stimulates the human alpha2(I) collagen gene expression. *J Invest Dermatol* **117**, 301-308.

Jamora, C., DasGupta, R., Kocieniewski, P. and Fuchs, E. (2003). Links between signal transduction, transcription and adhesion in epithelial bud development. *Nature* **422**, 317-322.

Jarvinen, E., Salazar-Ciudad, I., Birchmeier, W., Taketo, M. M., Jernvall, J. and Thesleff, I. (2006). Continuous tooth generation in mouse is induced by activated epithelial Wnt/beta-catenin signaling. *Proc Natl Acad Sci U S A* **103**, 18627-18632.

Jarvinen, E., Shimomura-Kuroki, J., Balic, A., Jussila, M. and Thesleff, I. (2018). Mesenchymal Wnt/beta-catenin signaling limits tooth number. *Development* **145**.

Kozawa, Y., Yokota, R., Chisaka, H., Yamamoto, H., Suzuki, K., & Elsey, R. M. (2005). Evagination and Invagination of the Oral Epithelium during Tooth Development in Alligator Mississippiensis. *Journal of Hard Tissue Biology, 14*(2), 170-171.

Lammi, L., Arte, S., Somer, M., Jarvinen, H., Lahermo, P., Thesleff, I., Pirinen, S. and Nieminen, P. (2004). Mutations in AXIN2 cause familial tooth agenesis and predispose to colorectal cancer. *Am J Hum Genet* **74**, 1043-1050.

Li, J., Chatzeli, L., Panousopoulou, E., Tucker, A. S. and Green, J. B. A. (2016). Epithelial stratification and placode invagination are separable functions in early morphogenesis of the molar tooth. *Development*.

Liu, F., Chu, E. Y., Watt, B., Zhang, Y., Gallant, N. M., Andl, T., Yang, S. H., Lu, M. M., Piccolo, S., Schmidt-Ullrich, R., et al. (2008). Wnt/beta-catenin signaling directs multiple stages of tooth morphogenesis. *Dev Biol* **313**, 210-224.

Liu, W., Shaver, T. M., Balasa, A., Ljungberg, M. C., Wang, X., Wen, S., Nguyen, H. and Van den Veyver, I. B. (2012). Deletion of Porcn in mice leads to multiple developmental defects and models human focal dermal hypoplasia (Goltz syndrome). *PLoS One* **7**, e32331.

Mammoto, T., Mammoto, A., Jiang, A., Jiang, E., Hashmi, B. and Ingber, D. E. (2015). Mesenchymal condensation-dependent accumulation of collagen VI stabilizes organ-specific cell fates during embryonic tooth formation. *Dev Dyn* **244**, 713-723.

Marin-Riera, M., Moustakas-Verho, J., Savriama, Y., Jernvall, J. and Salazar-Ciudad, I. (2018). Differential tissue growth and cell adhesion alone drive early tooth morphogenesis: An ex vivo and in silico study. *PLoS Comput Biol* **14**, e1005981.

Metscher, B. D. (2009). MicroCT for comparative morphology: simple staining methods allow high-contrast 3D imaging of diverse non-mineralized animal tissues. *BMC Physiol* **9**, 11

Morita, R., Kihira, M., Nakatsu, Y., Nomoto, Y., Ogawa, M., Ohashi, K., Mizuno, K., Tachikawa, T., Ishimoto, Y., Morishita, Y., et al. (2016). Coordination of Cellular Dynamics Contributes to Tooth Epithelium Deformations. *PLoS One* **11**, e0161336.

Murray, J. D. and Kulesa, P. M. (1996). On a dynamic reaction–diffusion mechanism: the spatial patterning of teeth primordia in the alligator. *J. Chem. Soc., Faraday Trans.* **92**, 2927-2932.

Neubüser, A., Peters, H., Balling, R. and Martin, G. R. (1997). Antagonistic Interactions between FGF and BMP Signaling Pathways: A Mechanism for Positioning the Sites of Tooth Formation. *Cell* **90**, 247-255.

Panousopoulou, E. and Green, J. B. (2016). Invagination of Ectodermal Placodes Is Driven by Cell Intercalation-Mediated Contraction of the Suprabasal Tissue Canopy. *PLoS Biol* **14**, e1002405.

Prochazka, J., Prochazkova, M., Du, W., Spoutil, F., Tureckova, J., Hoch, R., Shimogori, T., Sedlacek, R., Rubenstein, J. L., Wittmann, T., et al. (2015). Migration of Founder Epithelial Cells Drives Proper Molar Tooth Positioning and Morphogenesis. *Dev Cell* **35**, 713-724.

Sadier, A., Twarogowska, M., Steklikova, K., Hayden, L., Lambert, A., Schneider, P., Laudet, V., Hovorakova, M., Calvez, V. and Pantalacci, S. (2019). Modeling Edar expression reveals the hidden dynamics of tooth signaling center patterning. *PLoS Biol* **17**, e3000064.

Sasaki, T., Ito, Y., Xu, X., Han, J., Bringas, P., Jr., Maeda, T., Slavkin, H. C., Grosschedl, R. and Chai, Y. (2005). LEF1 is a critical epithelial survival factor during tooth morphogenesis. *Dev Biol* **278**, 130-143.

Shyer, A. E., Rodrigues, A. R., Schroeder, G. G., Kassianidou, E., Kumar, S. and Harland, R. M. (2017). Emergent cellular self-organization and mechanosensation initiate follicle pattern in the avian skin. *Science* **357**, 811-815.

Sick, S., Reinker, S., Timmer, J. and Schlake, T. (2006). WNT and DKK determine hair follicle spacing through a reaction-diffusion mechanism. *Science* **314**, 1447-1450.

Smith, M. M., Johanson, Z., Butts, T., Ericsson, R., Modrell, M., Tulenko, F. J., et al. (2015). Making teeth to order: conserved genes reveal an ancient molecular pattern in paddlefish (Actinopterygii). *Proc Biol Sci, 282*(1805).

Stricker, J., Falzone, T. and Gardel, M. L. (2010). Mechanics of the F-actin cytoskeleton. *J Biomech* **43**, 9-14.

Blume, S.W., Snyder, R.C., Ray, R., Thomas, S., Koller, C.A., Miller, D.M. (1991). Mithramycin inhibits Sp1 binding and selectively inhibits transcriptional activity of the dihydrofolate reductase gene in vitro and in vivo. *J Clin Invest*.

ten Berge, D., Koole, W., Fuerer, C., Fish, M., Eroglu, E. and Nusse, R. (2008). Wnt signaling mediates self-organization and axis formation in embryoid bodies. *Cell Stem Cell* **3**, 508-518.

Thesleff, I. and Sharpe, P. (1997). Signalling networks regulating dental development. *Mech Dev* **67**, 111-123.

Tokita, M., Chaeychomsri, W. and Siruntawineti, J. (2013). Developmental basis of toothlessness in turtles: insight into convergent evolution of vertebrate morphology. *Evolution* **67**, 260-273.

Tucker, A. S. and Sharpe, P. T. (1999). Molecular genetics of tooth morphogenesis and patterning: the right shape in the right place. *J Dent Res* **78**, 826-834.

Valenta, T., Hausmann, G. and Basler, K. (2012). The many faces and functions of beta-catenin. *EMBO J* **31**, 2714-2736.

van Roy, F. and Berx, G. (2008). The cell-cell adhesion molecule E-cadherin. *Cell Mol Life Sci* **65**, 3756-3788.

Wang, X.-P., O'Connell, D. J., Lund, J. J., Saadi, I., Kuraguchi, M., Turbe-Doan, A., Cavallesco, R., Kim, H., Park, P. J., Harada, H., et al. (2009). Apc inhibition of Wnt signaling regulates supernumerary tooth formation during embryogenesis and throughout adulthood. *Development* **136**, 1939-1949.

Wang, X. P. and Fan, J. (2011). Molecular genetics of supernumerary tooth formation. *Genesis* **49**, 261-277.

Widelitz, R. B., Jiang, T. X., Yu, M., Shen, T., Shen, J. Y., Wu, P., et al. (2003). Molecular biology of feather morphogenesis: a testable model for evo-devo research. *J Exp Zool B Mol Dev Evol, 298*(1), 109-122

Yu, T. and Klein, O. D. (2020). Molecular and cellular mechanisms of tooth development, homeostasis and repair. *Development* **147**.

3.1 Concluding Discussion

Developing mouse molars serve as an excellent model to study development of ectodermal organs because they are simple in structure, accessible and easy to culture *ex vivo*, allowing time-lapse imaging and pharmacological manipulation. Furthermore, dental organs undergo comparable developmental events to other ectodermal organs, such as those in development of hair follicles and feathers, making findings from tooth development studies of general interest to developmental biologists.

From a clinical perspective, teeth are vital for a healthy life. Unfortunately, in the Western world, it is estimated that 7% of adults lose at least one tooth by 17 years of age, and people over 50 years have 12 missing teeth on average (Sharpe et al., 2005). While dentures and dental implants have become common methods for restoring missing dentition, these therapies require preparation of adjacent healthy teeth or can fail due to limited osseointegration. As a result, increasing demands for biological replacement of missing teeth have encouraged research in bioengineering of the dental organ. One way to do this would be to develop an approach for regenerating the teeth by recreating the signaling networks that regulate odontogenesis. This requires a thorough understanding of odontogenic signaling pathways from the molecular to the organ level.

In my dissertation, I explored how Wnt signaling, which is indispensable for tooth development in the embryo and may offer potential avenues to build a tooth *de novo*,

regulates tooth development. Through loss-of-function and gain-of-function approaches, I investigated how the Wnt/β-catenin pathway guides dental epithelial and mesenchymal cells during the early stages of tooth development. While Wnt/β-catenin signaling has been widely studied in various developmental contexts, including tooth development, the lack of an adequate genetic tool to perturb Wnt/β-catenin pathway at specific times in specific tissues has imposed challenges in elucidating the role of the pathway in regulating cell behaviors during tooth development. To better understand the role of Wnt signaling in odontogenesis, I took a Cre/Lox mouse genetics approach, which utilized *Fgf8*-promoter-driven induction of *β-catenin* mutations to hyperactivate and inactivate the Wnt pathway in dental epithelium at the initiation stage. By doing so, I was able to understand the role of the Wnt pathway in the molar epithelium at the earliest stages of tooth development.

My results not only revealed that early Wnt/β-catenin signaling directs invagination vs. evagination of the dental epithelium, but also suggest that Wnt signaling is involved in a reaction-diffusion network that determine the presumptive sites of the molar tooth germ within the oral epithelium. While perturbing either molar epithelium or mesenchyme affects both cell types due to highly dynamic interactions between epithelium and mesenchyme reception of Wnt/β-catenin pathway may be required within the epithelium, because hyperactivating the same pathway in the mesenchyme yielded neither evagination nor ectopic formation of tooth germs.

In addition to exploring the role of Wnt/β-catenin in tooth development, I analyzed and compared observations on the mechanisms of tooth development made among different published studies in this dissertation. Interestingly, different conclusions on the same odontogenic process were drawn by different groups, perhaps owing to limitations in available techniques and analytic approaches in the field as explained in Chapter 1 of this thesis. I have provided potential explanations for these discrepancies, and I propose that exploring these possibilities in the future will improve our fundamental understanding of how the tooth is formed at a molecular and cellular level.

References

Sharpe, Paul T.Young, Conan S. "Test-Tube Teeth." Scientific American 293.2 (2005): 34-41. Military & Government Collection.

Publishing Agreement

It is the policy of the University to encourage open access and broad distribution of all theses, dissertations, and manuscripts. The Graduate Division will facilitate the distribution of UCSF theses, dissertations, and manuscripts to the UCSF Library for open access and distribution. UCSF will make such theses, dissertations, and manuscripts accessible to the public and will take reasonable steps to preserve these works in perpetuity.

I hereby grant the non-exclusive, perpetual right to The Regents of the University of California to reproduce, publicly display, distribute, preserve, and publish copies of my thesis, dissertation, or manuscript in any form or media, now existing or later derived, including access online for teaching, research, and public service purposes.

DocuSigned by:
Rebecca Yewon Kim
400C1E2D2FF44B7...
Author Signature

12/16/2021
Date